

WORKING FLUID SELECTION FOR AN INCREASED EFFICIENCY  
HYBRIDIZED GEOTHERMAL-SOLAR THERMAL POWER  
PLANT IN NEWCASTLE, UTAH

by

John Walter Carnell

A thesis submitted to the faculty of  
The University of Utah  
in partial fulfillment of the requirements for the degree of

Master of Science

Department of Chemical Engineering

The University of Utah

May 2012

Copyright © John Walter Carnell 2012

All Rights Reserved

The thesis of John Walter Carnell

has been approved by the following supervisory committee members:

Milind Deo , Member 3/2/2012  
Date Approved

and by JoAnn Lighty, Chair of  
the Department of Chemical Engineering

and by Charles A. Wight, Dean of The Graduate School.

## **ABSTRACT**

Renewable sources of energy are of extreme importance to reduce greenhouse gas emissions from traditional power plants. Such renewable sources include geothermal and solar thermal energy. These involve harnessing the heat from underground water sources or from solar irradiance. The heat energy is used to vaporize a working fluid which turns a turbine and generator system to produce electricity. The working fluid is then condensed and reused in the cycle. The working fluid needs to be carefully selected based on the geothermal brine temperature or the amount of solar irradiation available and the fluid's thermodynamic properties.

There are many low temperature geothermal resources that have the potential to generate commercial electricity, but due to their low temperatures cannot do so efficiently. The efficiency of geothermal power plants can be increased by adding solar energy. A commercially successful method of concentrating solar power is the solar trough. A solar trough is a parabolic mirror that focuses solar energy onto a collector tube. A heat transfer fluid is circulated within the tube to collect the energy. This heat transfer fluid would be heated and passed through a heat exchanger with the working fluid in a binary power plant to increase the working fluid's enthalpy.

There are vast quantities of solar irradiance data available for many locations throughout the United States. The data of interest are the direct normal irradiance which is measured by a pyrheliometer and a solar tracking device. Published data have shown that the direct normal radiation can be as high as  $1,000 \text{ W/m}^2$  during peak hours of the

day with a daily average, during sunlight hours, of  $850 \text{ W/m}^2$ . With these energy rates it could be advantageous to use this solar energy to increase the enthalpy of a power system. Specific measurements should be made at a geothermal site in order to know if such a project is feasible. If the project is feasible, a working fluid for the power cycle should be selected and an economic analysis should be performed in order to make project recommendations.

## TABLE OF CONTENTS

ABSTRACT .....	iii
LIST OF FIGURES .....	vii
LIST OF TABLES .....	ix
1. GEOTHERMAL OVERVIEW .....	1
1.1 Types of Geothermal Power Plants .....	1
1.1.1 Dry Steam Power Plant .....	1
1.1.2 Flash Plant .....	3
1.1.3 Binary Power Plant .....	4
1.2 Benefits of Binary Power Plants .....	6
1.3 Working Fluid .....	7
2. SOLAR THERMAL OVERVIEW .....	10
2.1 Concentrated and Collection Technologies .....	10
2.1.1 Power Tower .....	10
2.1.2 Stirling Dish .....	14
2.1.3 Parabolic Trough .....	16
2.2 Moving Solar Energy .....	18
2.2.1 Parabolic Trough – Reflectivity .....	19
2.2.2 Glass Envelope – Transmissivity .....	20
2.2.3 Receiver Tubes – Absorptivity .....	21
2.3 Heat Transfer Fluid .....	21
2.4 Maintenance .....	22
3. THERMODYNAMICS OF THE WORKING FLUID .....	23
3.1 T-s Diagrams and Types of Working Fluids .....	23
3.2 Power Cycles and P-h Diagrams .....	26
3.3 Carnot and Triangular Cycles .....	34
3.4 Thermal and Exergetic Efficiency .....	36
4. GEOTHERMAL AND SOLAR RESOURCE DATA .....	39
4.1 Geothermal Resource in Newcastle, UT .....	39

4.2 Preliminary Solar Testing and Measurements.....	42
4.3 Solar Resource in Newcastle, UT .....	48
5. HYBRID GEOTHERMAL-SOLAR THERMAL POWER PLANT .....	55
5.1 Design Considerations .....	55
5.2 Location and Minimizing the Footprint .....	58
5.3 Thermal Storage.....	60
5.4 Selection of Working Fluid .....	61
6. FEASIBILITY.....	63
6.1 Process Simulations .....	63
6.2 Resulting Thermodynamics and Efficiency .....	71
6.3 Recommendations for Newcastle Geothermal-SolarThermal Hybrid Plant .....	76
APPENDICES	
A. GEOTHERMAL RESOURCE .....	78
B. P-H AND Q-T DIAGRAMS .....	84
BIBLIOGRAPHY .....	91

## LIST OF FIGURES

1 - Schematic of a dry steam power plant.....	2
2 - Schematic of a flash power plant. ....	3
3 - Schematic of a binary power plant.....	5
4 - Frequency of geothermal temperatures. ....	5
5 - Schematic of power tower plant. ....	11
6 - Schematic of Planta Solar 10 .....	13
7 - Google Earth image of PS10 and PS20.....	13
8 - Steps in the process of a sterling engine.....	15
9 - Schematic of trough power plant. ....	16
10 - Focal point of a parabola. ....	19
11 - T-s diagram of water. ....	24
12 - T-s diagram of isobutane. ....	25
13 - Psychrometric chart at 101.325 kPa.....	29
14 - P-h diagram of the power cycle. ....	31
15 - T-q diagram for pinch point analysis. ....	34
16 - Carnot and trilateral efficiency. ....	36
17 - Conceptual model of the Newcastle Geothermal System .....	40
18 - Depiction of GHI (a), DHI (b) and DNI (c).....	42
19 - Magnetic declination of the United States.....	45
20 - Solar station set up at EGI. ....	46



21 - Solar Station in Ticaboo, UT .....	47
22 - Sunny day irradiance levels in Newcastle, UT. ....	50
23 - Mostly cloudy day irradiance levels in Newcastle, UT.....	50
24 - Cloudy day irradiance levels in Newcastle, UT.....	51
25 - Irradiance comparison between Newcastle and Cedar City on 11/26/2011. ....	51
26 - Schematic of hybrid geothermal-solar thermal power plant.....	56
27 - P-h diagram of hybrid power plant. ....	57
28 - P-h diagram of isobutane with lines of constant entropy. ....	58
29 - Geothermal and solar resources in Utah.....	59
30 - Promax configuration of geothermal-only scenario.....	64
31- Promax configuration of geothermal-solar thermal hybrid scenario. ....	68
32 - P-h diagram of isobutane in geo-only scenario.....	72
33 - q-T diagram for isobutane. ....	73
34 - Promax q-T diagram for isobutane. ....	73
35 - P-h diagram of isobutane in the hybrid scenario.....	74
36 - Latent heat and thermal efficiency. ....	75
A1 - Wells at Newcastle, UT .....	79
A2 - More well locations at Newcastle, UT. ....	80
A3 - Temperature-depth monitoring at well MN-6.....	81
A4 - Temperature-depth monitoring at well MN-7.....	82
A5 - Heat flow map of Newcastle, UT .....	83

## LIST OF TABLES

1 - Solar field and land area of SEGS plants. ....	17
2 - Working fluid selection criteria. ....	62
3 - Results of Promax simulation for geothermal-only scenario. ....	65
4 - Results of geo-only operation. ....	65
5 - Operating conditions of the hybrid geothermal-solar thermal power plant. ....	68
6 - Results of hybrid geothermal-solar thermal operation. ....	69
7 - Solar energy, solar field and land requirements.....	70
8 - Annual power production and land to power ratio. ....	70
9 - Annual power and thermal efficiency. ....	71
10 - Latent heat and thermal efficiency. ....	75

## **1. GEOTHERMAL OVERVIEW**

The word geothermal can be parsed into two words to understand its meaning; geo, meaning earth, and thermal, meaning heat. The concept of geothermal power production is to use the Earth's natural thermal energy to produce electricity. With increased concern about carbon dioxide emissions and pollution, there has been greater interest in green, renewable energy. This is where geothermal energy can be important. It produces extremely small amounts of carbon dioxide when compared to traditional coal or natural gas fired power plants. It is also considered base load power since it can operate continuously during the day and night.

### 1.1 Types of Geothermal Power Plants

There are three main types of geothermal power plants that are used to convert heat energy into electric energy. These are dry steam, flash and binary power plants. The type of power plant used at a specific site is determined by the geologic setting and the resource temperature.

#### 1.1.1 Dry Steam Power Plant

A dry steam power plant requires that only steam be produced from a geothermal well. This steam is cleansed of particulate matter and of any impurities that may have traveled to the surface by venting noncondensable gasses such as carbon dioxide and hydrogen sulfide. It is then sent to the turbine and generator system. Exhaust from the

turbine is commonly sent to a direct contact condenser. A direct contact condenser sprays cool water on the hot steam in order to turn the vapor into a hot liquid. The hot liquid then goes to the cooling tower where some of the water evaporates reducing the temperature of the water. The cooled water is then sent back to the direct contact condenser. Any accumulated liquid is injected back into the geologic formation in a location where the system is naturally recharged. Figure 1 shows a sketch of a dry steam power plant.

The first geothermal power plant was a dry steam plant located in Larderello, Italy. It was constructed in the early 20th century when Piero Ginori Conti first powered a  $\frac{3}{4}$  horsepower reciprocating steam engine with natural dry steam from a geothermal well to illuminate five light bulbs. In 1905 a 20 kW turbo alternator was installed in order to provide power to Conti's factory. This was the first time that electricity produced from geothermal energy was distributed industrially. In 1916 production was improved in order to provide 2,750 kW of electric power to the surrounding area. Not only is the Larderello field unique due to the fact that it is a dry steam reservoir, it is also considered the birthplace of geothermal energy production. Current annual production at the Larderello field is 4,800 GWh.

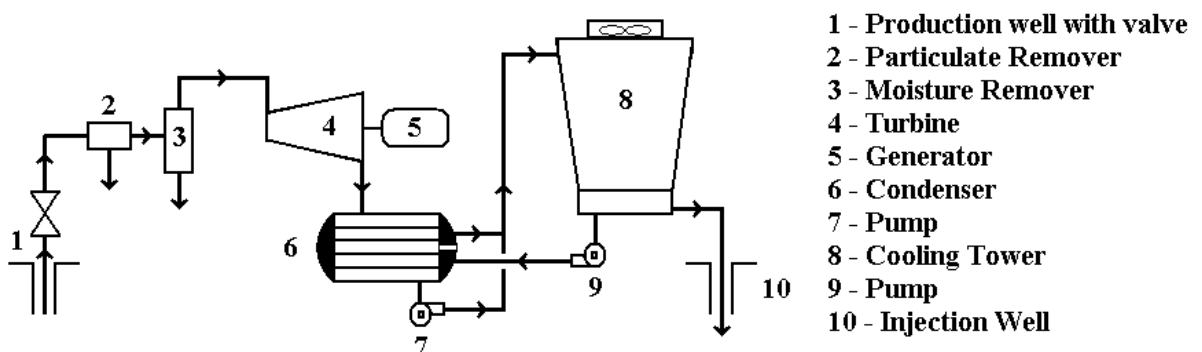


Figure 1 - Schematic of a dry steam power plant.

Another famous set of dry steam power plants is located in The Geysers geothermal field in northern California. William Bell Elliot discovered the field in 1847. Initially, the hot steam was only used for recreational purposes. It was not until 1960 when the first commercial power plant was constructed. In 1967 Unocal became the operator of the field. With the continuation of the development of the field there were a total of 23 power plants with an installed capacity of 2,043 MWe. Difficulties with the field maintenance mandated that some plants be disassembled and the installed capacity was reduced to 1,517 MWe which still provides power to approximately 1.1 million residents (Calpine, 2011).

### 1.1.2 Flash Plant

The second type of geothermal power plant is a flash plant. Figure 2 is a schematic of a flash power plant. This type of power plant differs from a dry steam plant in that the fluid brought to the surface is a two phase mixture of liquid and vapor water. A cyclone separator at the wellhead separates the vapor and liquid phases. The vapor is sent

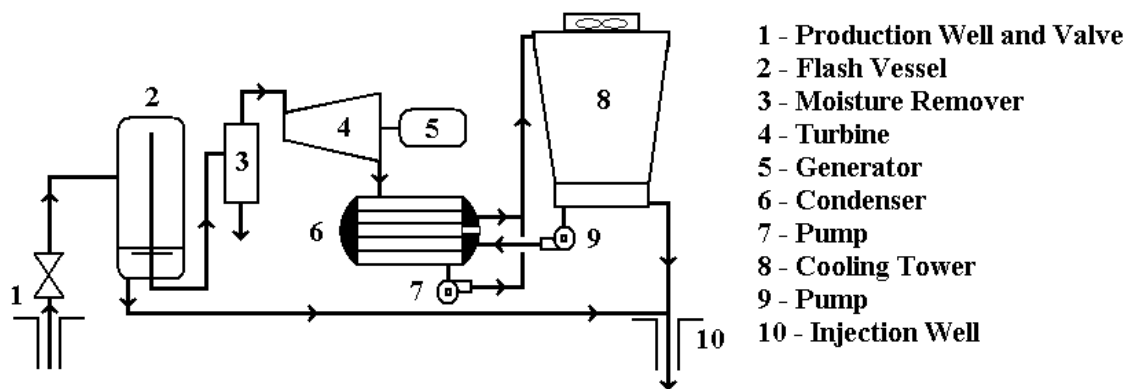


Figure 2 - Schematic of a flash power plant.

to the steam turbine and the remainder of the process is similar to that of a dry steam plant. Water from the well head separator is injected back into the formation along with the excess water from the cooling tower.

### 1.1.3 Binary Power Plant

The third method to utilize the geothermal energy is in a binary power plant. Binary power plants can use the lowest temperature resources to produce power. Geothermal brine temperatures can range from as low as 74°C (165°F) all the way up to approximately 150°C (302°F). Binary plants function very differently than dry steam or flash plants. Since the water is not hot enough to produce sufficient steam to run like a flash plant, it is used to boil a secondary working fluid such as light hydrocarbons or refrigerants. These working fluids are often used because they have a much lower boiling point than water. The working fluid is first boiled in the evaporator by the useful heat energy supplied by the geothermal brine. Once the working fluid is turned into the vapor phase it is sent to the turbine/generator system to extract useful power. Subsequently the working fluid is condensed back into the liquid phase. The liquid is then pumped to high pressure and is preheated by geothermal water exiting the evaporator. The geothermal water leaving the preheater is then injected back into the geologic formation and the working fluid is sent to the evaporator where it is boiled and the cycle starts again. Figure 3 is a schematic of a binary power plant.

Binary power plants can use the lowest temperature resource of the three types of power plants. Also, the majority of the known hydrothermal geothermal reservoirs have temperatures less than 150°C (302°F). Figure 4 shows a histogram of the frequency of

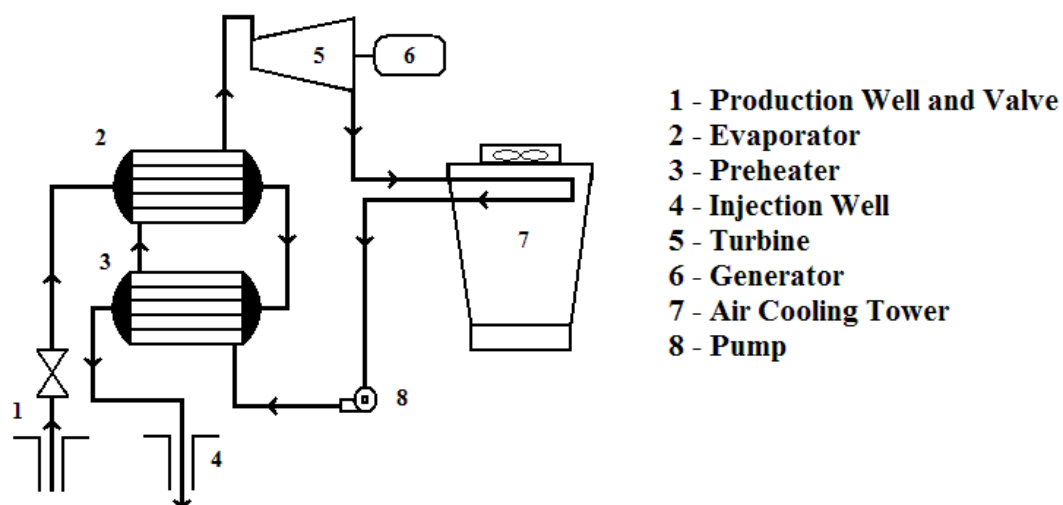


Figure 3 - Schematic of a binary power plant.

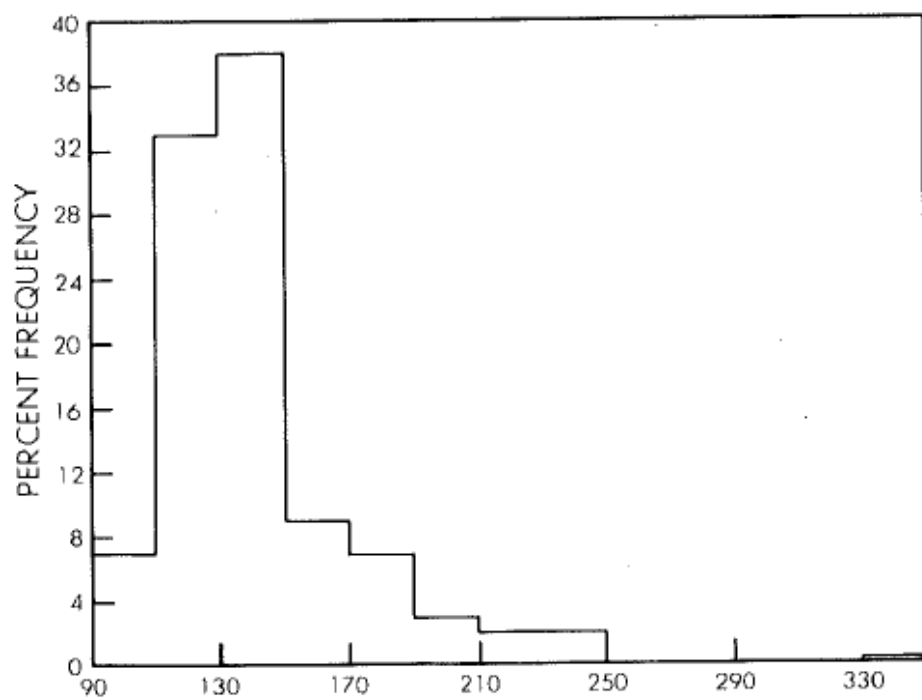


Figure 4 - Frequency of geothermal temperatures.

temperature of known hydrothermal resource temperatures. This chart was first published in the USGS circular 726 when the data were first collected. This gives great opportunity to the hybridized geothermal-solar thermal power plant because most of the known reservoirs have low temperatures. A binary cycle power plant could be constructed and augmented with solar thermal energy to produce power at increased efficiency.

### 1.2 Benefits of Binary Power Plants

There are some great advantages to binary power plants. In particular, binary power plant technology was developed for low-temperature geothermal systems. Chena Hot Springs, AK is a well-known example where there is low temperature geothermal power production in a binary power plant. At Chena Hot Springs the geothermal temperature resource is only 74°C (165°F). This is below the boiling point of water so it cannot produce steam to be used in a flash power plant. Chena Hot Springs uses binary power plant technology and r-134a was selected as the working fluid. This was selected because the boiling temperature is much lower than that of water (Resort, 2011).

There are still some emissions from dry steam and flash plants. They vent coproduced carbon dioxide and hydrogen sulfide into the atmosphere, albeit at a much lower rate than traditional coal or natural gas fired power plants. This is another aspect where binary power plants differ because all produced fluids, including carbon dioxide and hydrogen sulfide, are kept on a closed loop. This means that all produced carbon dioxide and hydrogen sulfide is injected back into the formation and none of these gasses are released into the atmosphere.



Binary power plants also have the flexibility of being either wet cooled or dry cooled. This refers to the functionality of the condenser. A wet cooled condenser has counter current direct contact with the warm water and air. The warm water will be cooled in accordance with the psychrometric chart to the wet bulb temperature as long as equilibrium can be achieved between the water and air. This will produce cool water and is best suited for dry, low relative humidity climates. This cool water is then used in the binary power plant to accept heat from the working fluid to condense it back into a liquid. Wet cooling towers need a water supply because some water is lost in the process. In locations where water is not as readily available, binary power plants can also be dry cooled. This means that they will use air as the medium to accept the heat being rejected from the power cycle. Ambient air temperature must be taken into consideration when designing a dry cooling system. The pressure of the working fluid can be altered in order to promote condensation at the ambient air temperature at the plant site.

### 1.3 Working Fluid

Appropriate working fluid selection for a binary power plant is critical. Selection of the working fluid must consider the resource temperature, condenser type and condenser operating temperature and the thermodynamic properties of the fluid. Some common working fluids used in binary geothermal power plants are isopentane, pentane, isobutane, r-134a and r-245fa. Specific criteria suggested for selecting a working fluid include toxicity of the fluid, stability under high temperature and pressure, boiling point, flash point, latent heat and thermal conductivity (Huang, 2010).

Of the criteria listed above, one of the most important is the boiling point of the working fluid. This is critical because there must be heat exchange between the geothermal brine and the working fluid with a sufficient temperature difference for efficient heat exchange and the working fluid must boil. The temperature at which boiling will occur can be altered by changing the pressure of the working fluid. Since an increase in pressure typically increases the boiling point of the working fluid an adjustment in pressure could allow a working fluid to be used at various evaporator temperatures. This allows a working fluid to be used at various geothermal resource temperatures.

There are some safety criteria listed, such as; toxicity, stability and flash point. Toxicity must be taken into account for safe plant operation. Also, if there were an emergency, there would be a written procedure to regain control in a safe manner. As previously mentioned, the pressure of the working fluid can be altered to have the fluid boil at a desired and designed temperature. In some cases these temperatures and pressures can be relatively high. Since some working fluids can break down, or decompose, at high temperatures and pressures fluid stability must be considered. Finally, the flash point is the lowest possible temperature at which a liquid can vaporize to form a mixture with air that will ignite. Although the flash point still requires an ignition source, it is a property that still must be considered when selecting a working fluid for a binary plant. The flash point must be known for safe operation of the facility.

Additional criteria are latent heat and thermal conductivity. These properties involve the amount of heat that is transferred from the geothermal brine to the working fluid. The thermal conductivity of a fluid is ability to conduct heat. The higher the thermal conductivity, the faster heat will conduct which will reduce the size of the heat

exchange equipment. It has been suggested that the latent heat of a working fluid should be high to enhance heat recover; however it seems that it should be low as to consume less heat energy in the power cycle. This will be investigated by process simulation and results will be given.

The binary power plant is the technology type that will be considered for the hybrid geothermal-solar thermal power plant. This technology is selected for two reasons; the geothermal reservoir at Newcastle, UT is of low temperature and binary power plant technology is the easiest to integrate additional heat energy.

## 2. SOLAR THERMAL OVERVIEW

Solar thermal power technologies use the heat energy of the sun in order to produce electricity. A common unit when referring to large amounts of energy is millions of tons of oil equivalent (Mtoe). The world's consumption of energy in 2010 was 12,852 Mtoe (Enerdata, 2012) which is 538 EJ<sup>1</sup>. The sun has a flux of 174 PW<sup>2</sup> on the Earth's atmosphere of which 30% is reflected leaving 121.8 PW to be absorbed by the Earth or 3,840,000 EJ annually. The amount of thermal energy the sun produces is more than 7,000 times the world's energy consumption in 2010. Simply put, the sun produces a large amount of energy that can be used for the power needs of the world.

### 2.1 Concentrated and Collection Technologies

One of the challenges with solar thermal technologies is gathering the solar energy and putting it to use by the most efficient means. The technologies that have been developed in order to do this are power towers, the Stirling dish and parabolic troughs. Each of these technologies will be discussed in further detail in the following section.

#### 2.1.1 Power Tower

The power tower system concentrates the sun's energy to a centralized location on the top of a tower. The energy is reflected by flat mirrors called heliostats. A two-axis

---

<sup>1</sup> 1 EJ is 1 Exajoule. 1 EJ =  $10^{18}$  J

<sup>2</sup> 1 PW is 1 Petawatt. 1 PW =  $10^{15}$  W

tracking system is required to ensure that the heliostats will reflect the irradiance to the central tower regardless of the path of the sun. A disadvantage of this type of power plant is that the reflective surface is not always normal to the sun; this reduces the effective area of the mirror. A favorable characteristic for this type of technology is that very high temperatures can be reached when an entire field of heliostats focuses all energy onto one location. As will be discussed in Chapter 3, the higher the temperature of the heat source, the higher the thermal efficiency with a given temperature sink. The concentrated solar energy is used to heat molten salt up to temperatures up to 1,022°F (550°C). This is used to boil water and superheat the steam. The temperature of the superheated steam can be as high as 932°F (500°C). The superheated steam is then sent to a turbine and generator system to produce power. Figure 5 is a simple schematic of the power tower system.

One of the first power tower pilot plants was the Solar One project. It was in operation from 1982-1988. The solar field was designed with 1,818 heliostats, each with an area of 40 m<sup>2</sup> (431 ft<sup>2</sup>) and the plant was designed to produce 10 MWe. What differs

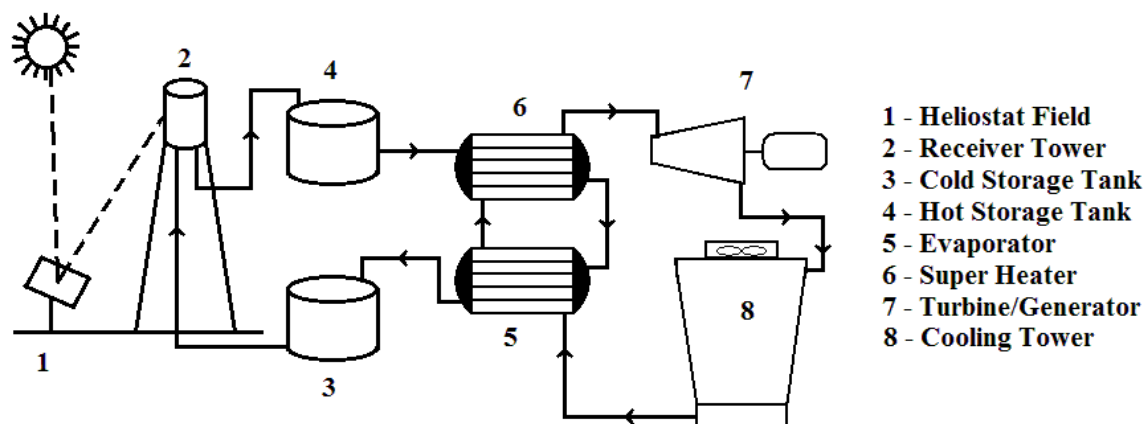


Figure 5 - Schematic of power tower plant.

from the schematic in Figure 5 is that the Solar One plant was designed with a direct steam generation concept, meaning that there was no molten salt involved. The receiver tower generated the steam which was then used in the turbine. It did have minimal thermal storage by way of heating thermal oil with excess steam which was used in the power generation cycle at times of intermittent cloud cover. The thermal storage system was only in operation until 1986 when it was damaged by a fire caused by water leaking into the hot oil tank (Kolb, 1991). Regardless, a great deal was learned from the operation of Solar One and when it was decommissioned in 1988, there were plans to convert Solar One into Solar Two. The conversion involved shifting some of the northern heliostats to the south, addition of 1,500 m<sup>2</sup> of heliostats, thermal salt energy storage and fossil fuel hybridization to heat the thermal salts. There would be 853,000 kg (1.88 million lbs.) of nitrate salt, 60% sodium nitrate and 40% potassium nitrate by weight (Reilly, 2001). This salt had a cold storage temperature of 550°F (288°C) and a hot storage temperature of 1022°F (550°C). The Solar Two project was decommissioned after approximately 10 years of operation in 1999 and converted into a Cherenkov Telescope in 2001 to measure gamma rays. (DeLaquil, 1991).

Planta Solar 10 (PS10) was the first commercial solar power tower. It was built near Seville, Spain and utilized the power tower technology developed by Abengoa Solar. PS10 is composed of 624 heliostats, each with an area of 120 m<sup>2</sup> (1,292 ft<sup>2</sup>), which focuses the sun's energy at the top of a 115 m (377 ft) tower and produces 11 MWe. The focused energy heats water to 250°C (482°F) at 40 bar (580 psi). This hot water is stored in tanks and when needed at the turbine, the pressure is reduced slightly to flash the water to steam. Figure 6 is a schematic of the PS10 power tower plant (Solucar, 2006).

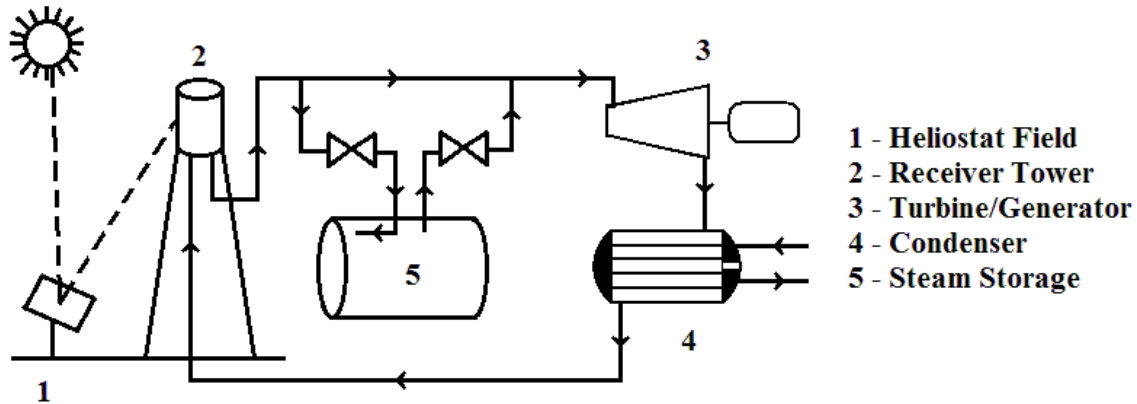


Figure 6 - Schematic of Planta Solar 10 (adapted from Solucar, 2006).

Abengoa Solar also built Planta Solar 20 (PS20) to the immediate west of PS10. Since 2009 it has been producing 20 MWe by concentrating the sun's energy from 1,255 heliostats each with an area of  $120 \text{ m}^2$  ( $1,292 \text{ ft}^2$ ) to the top of a 165 m (541 ft) tower. The heliostat configuration is denser in PS20. PS10 was constructed on 148 acres and PS20 was built on 210 acres giving a power to area ratio of 74.3 and 95.2 kW/acre respectively. Figure 7 is a satellite photograph of PS10 and PS20 (37.443888 North 6.259444 West).



Figure 7 - Google Earth image of PS10 and PS20. (Google, 2011)

With all that has been learned from Solar One and Solar Two, new ideas were implemented into the next generation of power towers. One such facility is currently under construction in Ivanpah, CA where a set of three power tower plants will be built with a total gross capacity of 392 MWe. This will be produced from 214,000 heliostats with a total area of 2,295,960 m<sup>2</sup> (24.7 million ft<sup>2</sup>). This project was originally scaled for 440 MWe but was reduced to afford preservation of the desert tortoise's habitat (BrightSource, 2011).

### 2.1.2 Stirling Dish

The solar Stirling dish is based on the workings of a Stirling engine with concentrated solar energy as the heat source. There are various configurations for this engine; the alpha type will be described here. The alpha type Stirling engine is composed of two pistons and cylinders that are set 90 degrees from each other and both have shafts connecting to a flywheel (Figure 8). One of the cylinders is designated as the hot piston and the other is the cold cylinder. The sun's energy is concentrated by a reflective dish that is similar in appearance to a satellite dish. This reflected energy serves as the fuel source for the hot cylinder which drives the engine. The hot and cold cylinders are connected so that a gas, or working fluid, can pass from one to the other and back again without leaking to the atmosphere. Where all of the gas is cool there is a minimum volume, since a cold gas has a smaller volume than a warm gas, and all of the working fluid enters the hot cylinder as seen in Figure 8a. The fuel source, in this case the sun, heats the working fluid and it expands and transfers back to the cold cylinder driving the fly wheel, Figure 8b. The cold cylinder is constructed to promote heat transfer to the



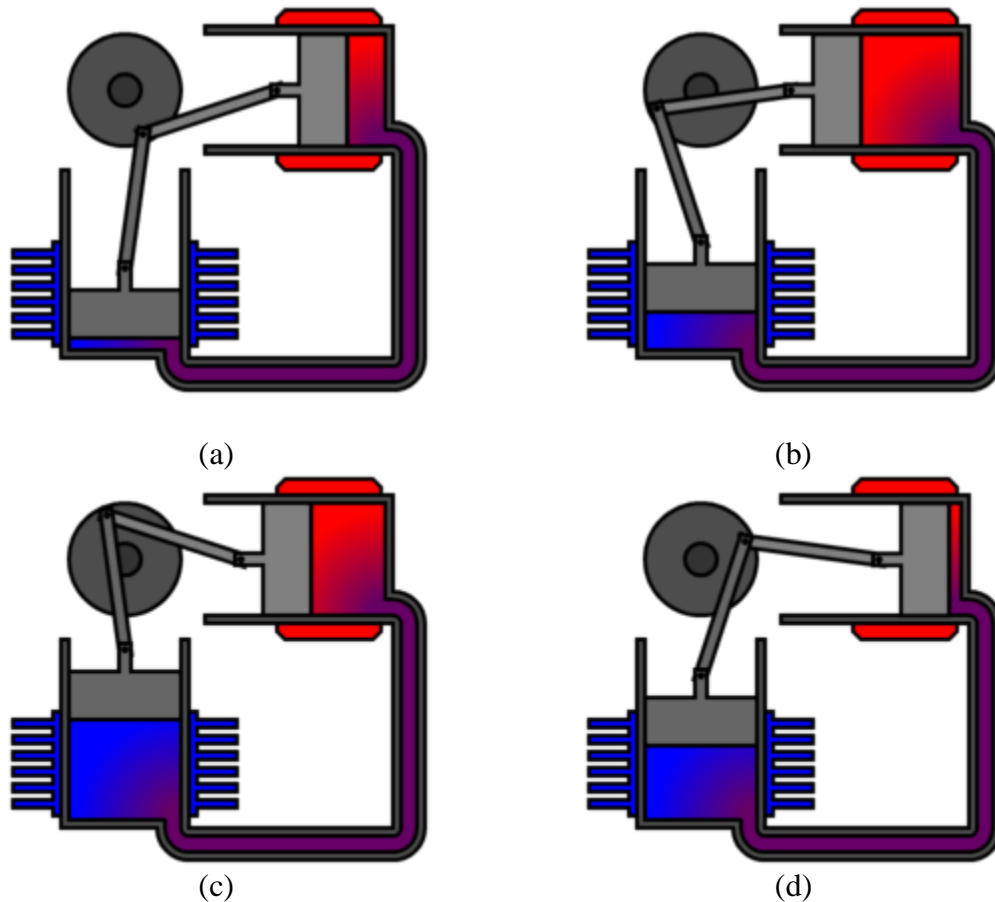


Figure 8 - Steps in the process of a sterling engine. Images by Richard Wheeler, used with permission (Wheeler, 2007)

surroundings, cooling the working fluid and contracting it, Figure 8c. The momentum in the fly wheel moves the cool gas back to the hot cylinder to be heated and expanded again, restarting the process; as shown in Figure 8d (Kongtragool, 2003). Figure 8 shows all four steps in this process.

Of the concentrating solar power technologies, the solar Sterling dish is one of the least common and is still being developed. The Maricopa Solar Project is a set of 60 Stirling dishes each with a capacity of 25 kWe giving a total generating capacity of 1.5 MWe. Some dish and engine systems are still being tested and developed at Sandia National Laboratory (National Renewable Energy Laboratory, 2010).

### 2.1.3 Parabolic Trough

A parabolic trough power plant operates in a manner similar to the power tower plant, with the difference being in the set-up of the solar field. The solar field of a trough plant is made up of parabolic mirrors. Each mirror has an absorber tube at its focal point. The sun's energy is reflected off of the mirrors, passes through a glass envelope and strikes the absorber tubes. A vacuum is maintained within the glass envelope to prevent convective heat losses. The absorber tubes are coated with a material that absorbs the majority of the energy that hits them. A heat transfer fluid (HTF) flows through the absorber tube. This fluid is typically composed of synthetic oils that have very low vapor pressure. The low vapor pressure enables the fluid to be heated to very high temperatures without rupturing the tubes. The hot oil is used to boil and superheat water at high temperature and pressure which is then sent to a steam turbine and generator system. The turbine exhaust is then condensed into a liquid by conventional cooling methods. Figure 9 is a general schematic of a parabolic trough power plant.

A series of nine trough power plants were built from 1984-1990 in the Mojave desert of California; these were called the Solar Electric Generating Systems (SEGS).

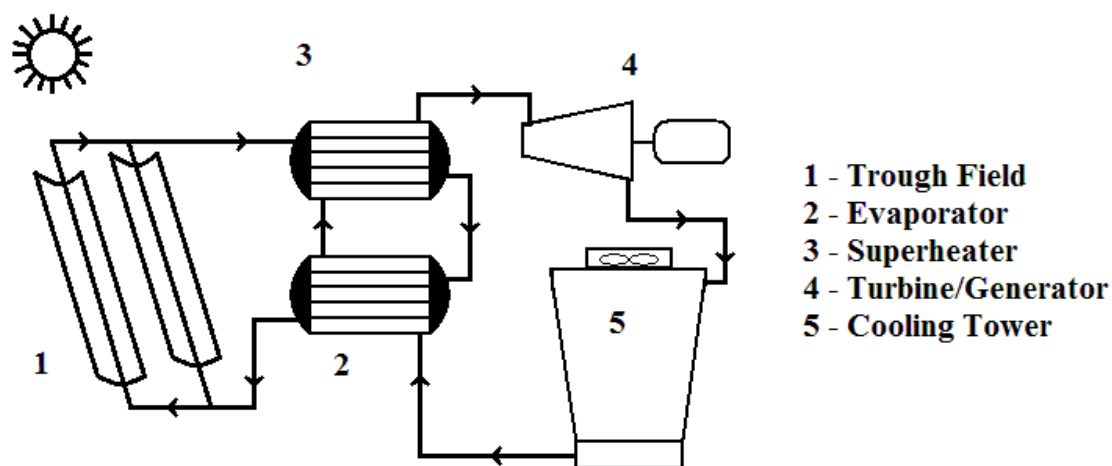


Figure 9 - Schematic of trough power plant.

Units I and II are located in Daggett, CA, units III-VII are in Kramer Junction, CA and units VIII and IX are located in Dry Harper Lake, CA. These plants were built to develop solar trough technology. Progressively, as each unit was built the working fluid's pressure and temperature were both increased. This was partially because the temperature of the heat transfer fluid was also increased so that higher-pressure water could be vaporized. The turbine capacity of the first unit is 13 MWe, units II-VII can deliver 30 MWe and the final two units have a capacity of 80 MWe. Table 1 shows the solar field area and land area of each of the units (Fernandez-Garcia, 2010).

Spain is one of the leading countries in developing and implementing solar technology. This is not surprising since the southern part of Spain has an annual average irradiance of approximately 2,200 kWh/m<sup>2</sup>/year (European Commission Joint Research Centre, 2007). The Spanish government has subsidized construction of solar thermal power plants, for example, the previously discussed Planta Solar 1 and 2 power tower facilities near Seville. In addition to these two power tower plants, many parabolic trough plants have been also built in Spain, notably the Andasol and Solnova projects.

Table 1 - Solar field and land area of SEGS plants.

Unit	Solar Field (m <sup>2</sup> )	Land Area (Acres)	Land Area (mi <sup>2</sup> )
I	82,960	29	0.05
II	190,338	67	0.10
III	230,300	80	0.13
IV	230,300	80	0.13
V	250,500	87	0.14
VI	188,000	66	0.10
VII	194,280	68	0.11
VIII	464,340	162	0.25
IX	483,960	169	0.26

One of the most recently constructed parabolic trough plants is the Nevada Solar One project in Boulder City, NV. The Spanish company Acciona began construction of this plant in February 2006 and power was being produced in July of the following year. The target design for electrical output was 64 MWe, but can produce up to 72 MWe net. This facility has been a major breakthrough in concentrating solar power technologies in the United States. No other plants have been built since the SEGS complex in the mid to late 1980s besides Nevada One Solar. Power plants that have been announced or are already under construction include the power towers at Ivanpah, CA, and two parabolic trough plants being constructed by the Spanish company, Abengoa Solar, Solana Generating Station and the Mojave Solar Park.

Of the available technology, the one selected for the geothermal-solar thermal power plant is the solar trough. This technology was selected because it has been proven at other facilities and the heat energy collected by the heat transfer fluid can be easily integrated with the process equipment of a binary power plant by heat exchanger.

## 2.2 Moving Solar Energy

Within this thesis the parabolic troughs are considered as the concentrating solar power technology that will be utilized. This section provides more specifics on how the solar energy is concentrated, captured and utilized in the power production process. In general, it occurs by being reflected and concentrated, transmitting through glass and being absorbed and moved by a heat transfer fluid.

### 2.2.1 Parabolic Trough – Reflectivity

Outside of the Earth's atmosphere the solar irradiance is estimated to be  $1386 \text{ W/m}^2$ . Since some of this energy is reflected back into space and some is absorbed within the atmosphere roughly  $1000 \text{ W/m}^2$  strikes the Earth's surface at peak hours. This radiant energy can be concentrated and collected at a parabolic trough's focal point. This point can be simply found by Equation 1.

$$f = x^2 / 4a \quad (1)$$

In this equation  $f$  is the distance from the vertex of the parabola on a line normal to the parabola's surface to the focal point,  $x$  is the radius of the open end of the parabola and  $a$  is the depth of the parabola. Figure 10 shows these dimensions.

Reflectivity is a property that determines the fraction of irradiance that is reflected by a given surface (Incropera, 2007). It is appropriate to construct solar troughs with a material with a reflectivity as close to one as possible in order to maximize the amount of

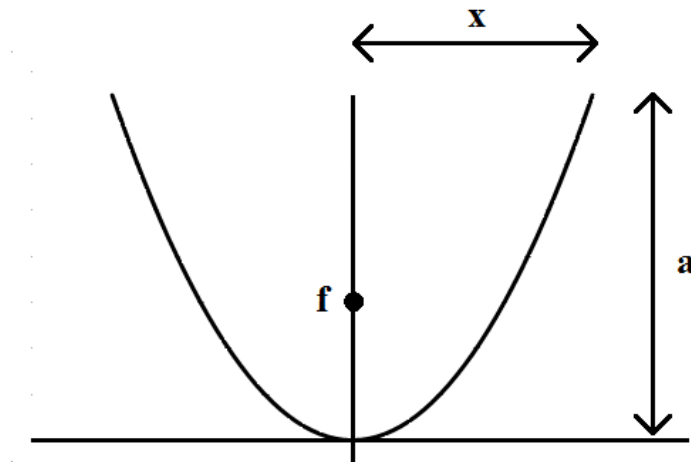


Figure 10 - Focal point of a parabola.

energy that can be collected. In a typical industrial situation, the EuroTrough-150 (ET150) solar trough uses mirrors that have a reflectivity of .94 meaning that 94% of solar irradiance that strikes the surface of the trough will be reflected to its focal point (Montes, 2009). This value is much greater than common mirrors which typically have a reflectivity closer to 0.7. If the irradiance is not reflected by the mirrors surface it likely absorbed into the mirror.

### 2.2.2 Glass Envelope – Transmissivity

After being reflected by the surface of the trough, the energy is focused onto the receiver tube. A glass envelope on the outside of the receiver tube must allow the majority of the energy to pass through it, implying high transmissivity. Transmissivity is a material property defined as the fraction of irradiance that is allowed to pass through it compared to the total amount of irradiance striking it. The ET150 uses a glass tube that has transmissivity of 94.5% (Montes, 2009).

The purpose of the glass envelope is to enclose the absorber tube within an evacuated volume. This maximizes the solar irradiance that is absorbed while at the same time minimizing convective loss. Forristall's calculations showed that the evacuated glass tube is extremely important (Forristall, 2003). Even though the absorber tube will be heated to very high temperatures the vacuum minimizes convective losses to the surroundings since there is little to no medium by which the heat energy can be transferred. For this reason, the glass enclosing the absorber tube must be highly transmissive, such as the glass used in the ET150.

### 2.2.3 Receiver Tubes – Absorptivity

Heat transfer fluid flows through the absorber tube which itself is within the glass envelope. With this component, the relevant criterion is absorptivity which is the fraction of irradiance that is absorbed by a surface (Incropera, 2007). A highly absorbent coating on the absorber tube maximizes the amount of energy transferred to the heat transfer fluid. The absorptivity of the tubes used in at the ET150 trough is .94. These tubes must be made of a material that can withstand extremely high temperatures of up to 400°C (752°F).

## 2.3 Heat Transfer Fluid

After the sun's energy is reflected from the surface of the trough, transmitted through the glass envelope and absorbed by the absorber tube, it conducts through the absorber tube wall and is transferred by convection into the heat transfer fluid (HTF). The appropriate heat transfer fluid is selected based on properties that include cost, safety, heat capacity and vapor pressure. Vapor pressure is the more important thermal property. With a greater heat capacity, the fluid transfers more energy without a substantial change in temperature. It is best for the vapor pressure to be low so that the heat transfer fluid can be heated to very high temperatures without having to increase the thickness of the absorber tubes significantly minimizing cost.

Therminol VP-1 is the heat transfer fluid that is used at the majority of the SEGS facilities. Units II-IX at the SEGS plants have HTF outlet temperatures ranging from 321-391°C (610-736°F). Therminol VP-1 under liquid conditions has an operating temperature in the range of 12-399°C (54-750°F) (Solutia, 2012).

## 2.4 Maintenance

One of the greatest advantages of parabolic trough plants is that their operating and management costs are very low when compared to coal-fired power plants. With that being the case, one of the greatest costs in maintaining a trough plant is cleaning the mirrors. The greatest problem with the collection of dirt or clays on the mirrors is not the reduction in reflectivity, but the scattering of energy. Dirt on the surface of the mirrors changes the path of the reflected energy so that it does not strike the absorber tube, therefore causing a loss in collected energy. To minimize the size of the solar field, the troughs must be kept clean. Similarly, the glass tubes must also be kept clean. When all of the concentrated energy strikes the glass tubes, impurities can scatter the energy. This necessitates a larger solar field to obtain the same amount of thermal energy as a smaller, clean field. It has been suggested that the mirrors and glass tubes be cleaned with either just water or with a diluted mild detergent followed immediately by a rinse. If a detergent is used, it must not be allowed to dry on any surface of the trough or glass envelope. Water with high amounts of dissolved solids must not be used in cleaning the mirrors and tubes to avoid water spots being formed on any surface. To prevent the formation of water spots, the water must be treated or purified by a water softener, deionization unit or reverse osmosis. The cost of each of these cleaning methods, and required frequency of cleaning, should be considered and is one of the major costs in maintaining a solar thermal power plant.



### 3. THERMODYNAMICS OF THE WORKING FLUID

When designing a binary type power plant, selection of the working fluid can make or break the project. As briefly discussed in Chapter 1, there are many considerations that must be taken into account when selecting a working fluid. This chapter will discuss some of the important thermodynamic properties of working fluids, maximum efficiency principles and efficiency.

#### 3.1 T-s Diagrams and Types of Working Fluids

A thermodynamic cycle can be outlined on a temperature-entropy diagram. From the second law of thermodynamic Equation 2 can be proven.

$$dQ = T \cdot ds \quad (2)$$

In this equation Q is heat energy, T is temperature and s is specific entropy. Equation 2 can be integrated to give Equation 3.

$$\Delta Q = T \cdot \Delta s \quad (3)$$

In Equation 3  $\Delta Q$  is the difference in heat between two specific states of the thermodynamic process,  $T$  is temperature and  $\Delta s$  is the difference in specific entropy of two specific states of the thermodynamic process. The significance of Equation 3 is that the total amount of heat transferred to the system can be calculated by knowing the area enclosed area in T-s diagram.

A second application of the T-s diagram is to determine whether the working fluid is wet or dry. The saturation curve on the T-s diagram is constructed from the temperature and specific entropy of a fluid at its boiling temperature; the fluid is changing from a liquid to a gas. As the pressure increases, the boiling temperature will change, which also changes the entropy. Figures 11 and 12 show T-s diagrams for water and isobutane.

On each of the diagrams in Figures 11 and 12, the region inside the curve is characterized as two-phased whereas there is only one phase – liquid or vapor outside of it. The critical point of the fluid is on the curve at the occurrence of the maximum

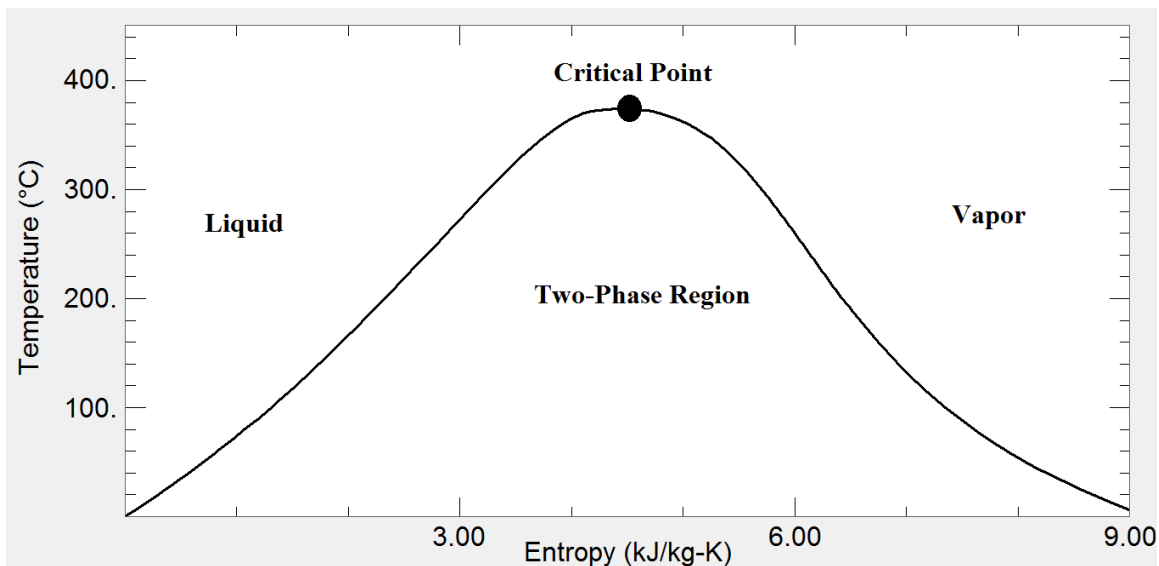


Figure 11 - T-s diagram of water.

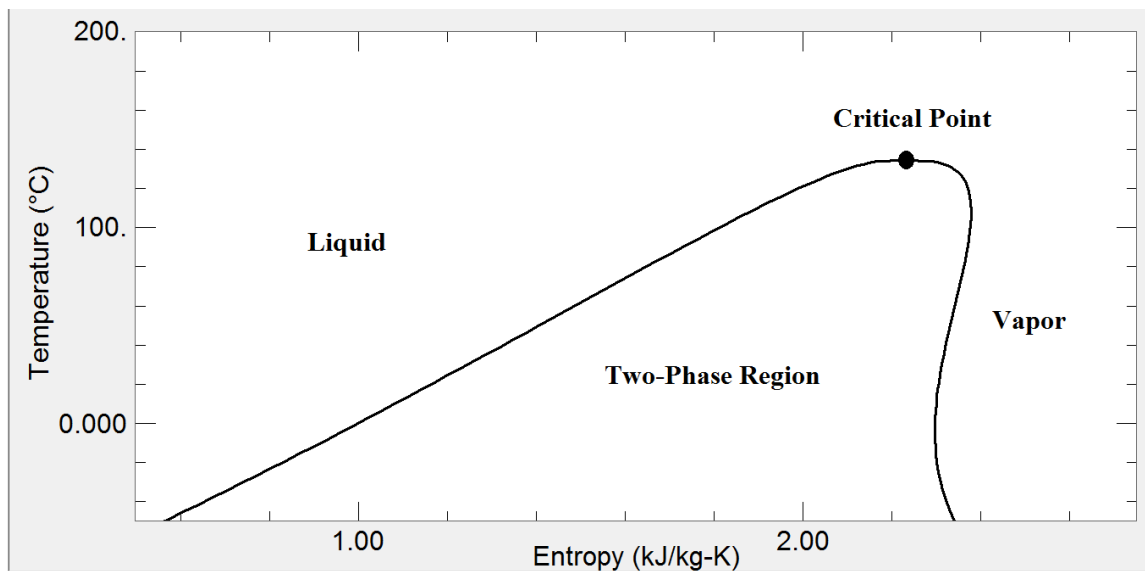


Figure 12 - T-s diagram of isobutane.

temperature. At this point there is no distinction between the liquid and vapor phases. The single phase region is separated into liquid and vapor phases, with the liquid phase to the left of the critical point and the vapor phase to the right.

The slope of the vapor saturation curve can be useful in plant design. For example, the T-s diagram water shown in Figure 11, the slope at any point on the saturated vapor side of the two-phase envelope is negative. This classifies water as a wet working fluid; if a power cycle turbine inlet uses saturated water vapor, it will condense when the temperature drops at constant entropy. On the other hand, above 0°C isobutane, as seen in Figure 13, has a positive slope in the area of saturated vapor. This means that there will be no condensation in the turbine when the temperature drops. The full power cycle is explained from thermodynamics viewpoint in the following section.

### 3.2 Power Cycles and P-h Diagrams

There are four major pieces of equipment that are involved in a power cycle; the turbine, condenser, pump and evaporator. Consider the power cycle for a binary power plant with a refrigerant or hydrocarbon as the working fluid. At the inlet of the turbine, the working fluid will be in the vapor phase at high pressure. By energy balance, and neglecting the potential and kinetic energy terms, the turbine extracts the useful energy from the working fluid by taking the difference in enthalpy at inlet and outlet of the turbine, as shown in Equation 4.

$$\dot{W}_t = \dot{m}_{wf}(h_1 - h_2) \quad (4)$$

In this equation  $\dot{W}_t$  represents work rate being extracted from the system,  $\dot{m}_{wf}$  is the working fluid mass flow rate and  $h$  is enthalpy. Subscript 1 represents the inlet conditions at the turbine while subscript 2 represents the outlet conditions.

The work rate is the maximum rate output for the turbine with the given thermodynamic properties of the working fluid. At times, a turbine is given an isentropic efficiency. If the work done in the turbine was reversible and there was no heat loss, the difference in entropy would be zero. In a real process that is not reversible, where there may be heat loss, the entropy increases. By assuming an isentropic efficiency,  $\eta_t$ , typically 85%, and equating the work terms in Equations 4 and 5, the thermodynamic state at the outlet of the turbine and total work can be calculated.

$$\dot{W}_t = \dot{m}_{wf}\eta_t(h_1 - h_{2s}) \quad (5)$$

In Equation 5 all of the symbols have the same meaning as in Equation 4.  $\eta_t$  is the isentropic efficiency of the turbine and  $h_{2s}$  is the enthalpy at the exit conditions of the turbine with the same entropy as in the inlet conditions. If a turbine operated at 100% isentropic efficiency, it would generate the maximum amount of work for the given conditions at the inlet and outlet.

After the working fluid exits the turbine, it must be condensed back into the liquid phase in the condenser. By a simplified energy balance the amount of heat energy that will need to be removed from the working fluid per unit mass is the difference in enthalpy at the outlet of the turbine with that of the working fluid in the liquid phase. Equation 6 shows the total cooling load for the condenser.

$$Q_{cond} = \dot{m}_{wf}(h_2 - h_3) \quad (6)$$

In this equation  $Q_{cond}$  is the rate that heat must be removed from the system,  $\dot{m}_{wf}$  is the mass flow rate of the working fluid,  $h_2$  is the outlet enthalpy of the turbine and  $h_3$  is the enthalpy of the working fluid at saturated liquid conditions. The flow rate of the cooling fluid can be calculated by equating the  $Q_{cool}$  terms in Equations 6 and 7 and solving for  $\dot{m}_{cool}$ .

$$Q_{cool} = \dot{m}_{cool}c_{avg}(T_a - T_b) \quad (7)$$

In Equation 7  $Q_{cool}$  is the required cooling rate,  $\dot{m}_{cool}$  is the mass flow rate of the cooling fluid,  $T_a$  is the inlet temperature of the cooling fluid and  $T_b$  is the outlet temperature of

the cooling fluid.  $Q_{\text{cool}}$  will be equal and opposite of  $Q_{\text{cond}}$ . In order to keep the size of the condenser to a minimum, it would be ideal to use water as the cooling fluid since it has superior heat transfer properties when compared to air. When water is used as the cooling fluid, after it has accepted the heat rejected by the working fluid, it would typically be sent to a cooling tower. The water is then passed by counter current flow of air allowing some evaporation which cools the water for reuse in accepting heat from the working fluid. If thermodynamic equilibrium can be achieved with the air, the warm water will cool in accordance to an energy balance shown by the psychrometric chart in Figure 13. The dry bulb temperature on the abscissa represents the temperature as measured by a thermometer. Relative humidity represents the percentage of the maximum amount of water that can be evaporated into the air. As the temperature of the air increases, so does its capacity to hold water vapor. The wet bulb temperature is indicated on the 100% relative humidity curve. The wet bulb temperature is the temperature of water in equilibrium with dry air. Consider an example; if the ambient air temperature is 20°C (68°F), the relative humidity is 30% and thermodynamic equilibrium has been achieved between the water and the air, the water would cool to a temperature of approximately 11°C (52°F). In arid climates, water is a precious resource and is often not used as the cooling fluid in geothermal power plants and air is used instead. In this case, the mass flow rate would be much greater because the temperature difference and heat capacity of air are much lower than for water. After the working fluid is cooled to the saturated liquid state, it must be pumped back to high pressure. By the simplified energy balance the work required by the pump can be simplified to the value determined in Equation 8.

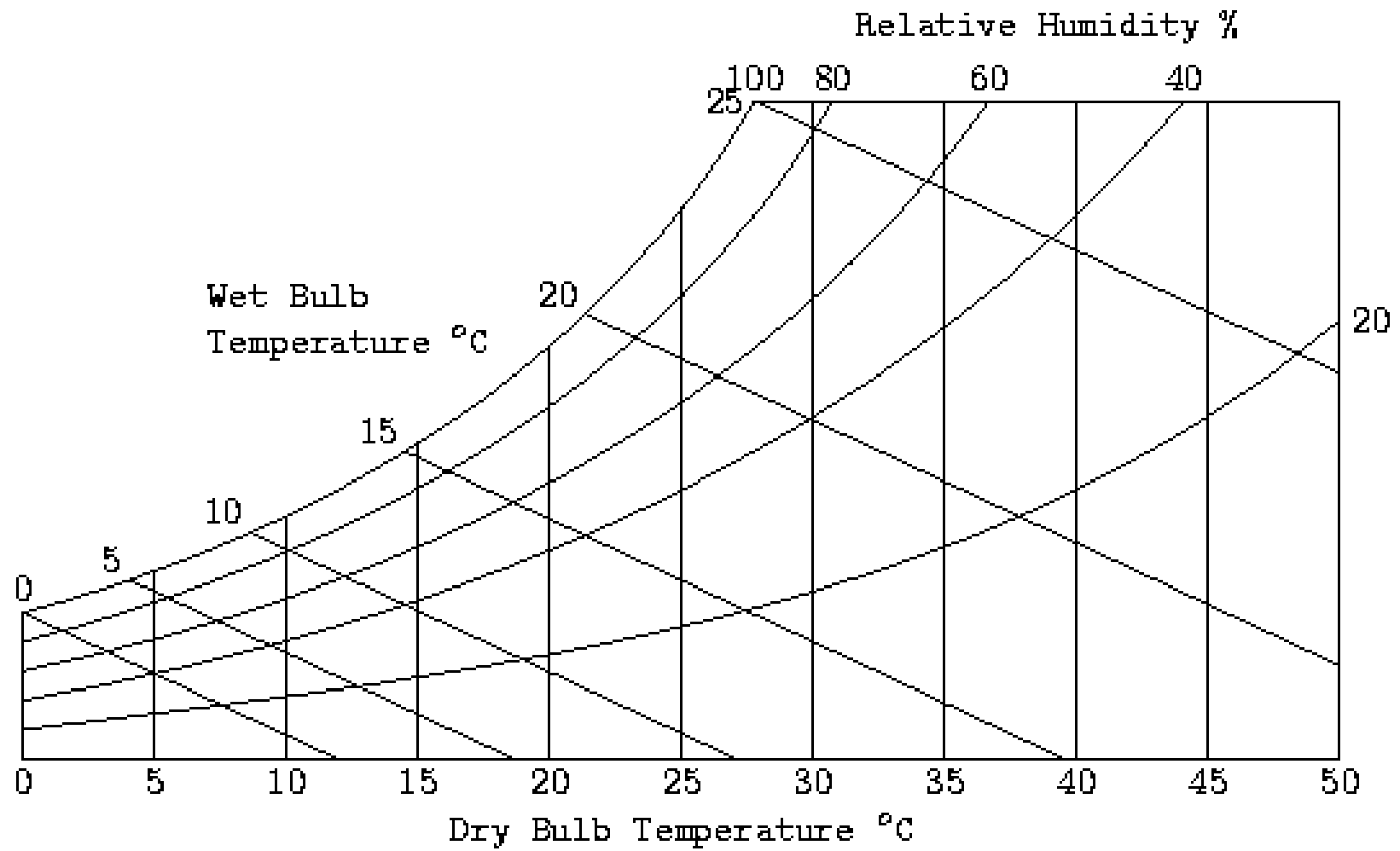


Figure 13 - Psychrometric chart at 101.325 kPa

$$\dot{W}_p = \dot{m}_{wf}(h_4 - h_3) \quad (8)$$

$\dot{W}_p$  is the work rate of the pump required by the system,  $\dot{m}_{wf}$  is the mass flow rate of the working fluid,  $h_3$  is the enthalpy of the working fluid in the saturated liquid phase and  $h_4$  is the enthalpy of the working fluid in the liquid phase at high pressure. Similar to the turbine, the pump also has an isentropic efficiency  $\eta_p$ . If there is no heat loss and the work is reversible, the isentropic efficiency would be 100% and the pump work equation would be given by Equation 9.

$$\dot{W}_p = \dot{m}_{wf}\eta_p(h_{4s} - h_3) \quad (9)$$

Equation 9 is similar to Equation 8 with the exception of the added isentropic pump efficiency term and using  $h_{4s}$  rather than  $h_4$ ,  $h_{4s}$  has the same entropy as that of  $h_3$ . By assuming the isentropic efficiency, the thermodynamic state and total work of the pump can be calculated.

After the fluid is pumped back up to high pressure, it must be preheated and evaporated before being sent back to the turbine. This preheating and evaporation can be done by a variety of heat sources including geothermal brines and solar heat transfer fluids. The pressure to which the fluid should be pumped will depend on the temperature of the heat source. The total amount of heat energy required can be described by Equation 10.

$$Q_{hot} = \dot{m}_{wf}(h_1 - h_4) \quad (10)$$



In this equation  $Q_{\text{hot}}$  is the amount of heat required by the working fluid to boil,  $\dot{m}_{\text{wf}}$  is the mass flow rate of the working fluid,  $h_1$  is the enthalpy of the working fluid at the inlet conditions of the turbine and  $h_4$  is the enthalpy of the working fluid after being pressurized by the pump. After the working fluid is pressurized and evaporated, it is then returned to the turbine to be reused in the power cycle. In equations 4 through 10 the sign conventions were arranged so all work and heat values would be positive which is why it was specified if the heat or work was being extracted or entering the system. Some engineering text books and journal articles may have a different sign convention and a detailed energy balance should be performed when designing a power cycle. Figure 14 shows the entire power cycle drawn on a P-h diagram and is for illustrative purposes and does not reflect actual calculations.

A pinch point analysis should also be done for the condenser, preheater and evaporator to ensure efficient heat transfer. From the pinch point analysis the required

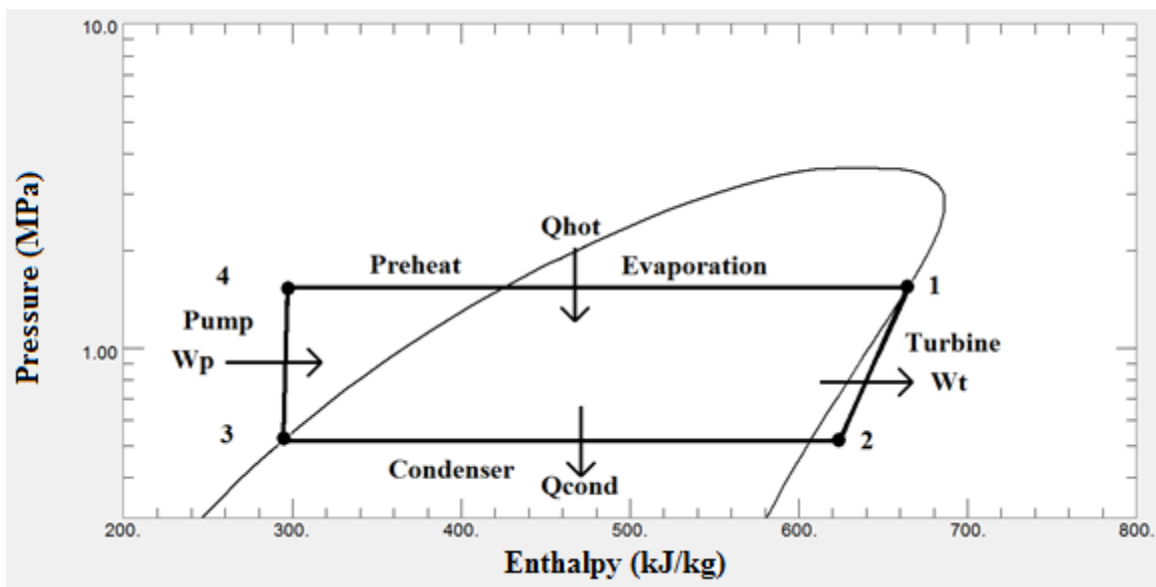


Figure 14 - P-h diagram of the power cycle.

mass flow rate of the working fluid can be obtained for a particular heat source. The first requirement is to know or estimate the heat source flow rate and temperature. When using geothermal brine as the heat source, the temperature of the brine only needs to be lowered to a temperature which does not allow precipitation of any dissolved solids. This needs to be confirmed by geochemical analysis of the fluids to quantify dissolved solids in the brine. Well testing should have also been done to know the approximate flow rate of the brine. Once this information is known, the temperature-heat transfer (T-q) diagram, in conjunction with an energy balance can be used to calculate the maximum flow rate of the working fluid. Equation 11 is a simplified energy balance between the working fluid and the geothermal brine.

$$\dot{m}_{wf}(h_1 - h_4) = \dot{m}_{geo}c_{avg}(T_x - T_y) \quad (11)$$

In Equation 11  $\dot{m}_{wf}$  is the mass flow rate of the working fluid,  $h_1$  is the enthalpy of the working fluid at the turbine inlet conditions,  $h_4$  is the enthalpy of the working fluid after it exits the pump,  $\dot{m}_{geo}$  is the mass flow rate of the geothermal brine,  $c_{avg}$  is the brine's average heat capacity over the temperature range from the hot temperature,  $T_x$  to the cold temperature  $T_y$ . Equation 11 can be solved to calculate the mass flow rate of the working fluid when the flow rate of the geothermal brine and temperatures are known. After the mass flow rate of the working fluid is known, the pinch point analysis can be performed. In the analysis, it is necessary to calculate the amount of heat energy required to increase the enthalpy of the working fluid from the conditions at the outlet of the pump to saturated liquid conditions. The percentage of heat transferred in preheating the working

fluid can then be calculated from the total amount of heat transferred in preheating and evaporating the working fluid. Once this is done, the pinch point temperature in the geothermal brine can be calculated by Equation 12 to ensure that the heat transfers from the geothermal brine to the working fluid at all times.

$$T_z = (T_x - T_y) \cdot x + T_x \quad (12)$$

In this equation  $T_z$  is the pinch point temperature in the geothermal brine,  $T_x$  is the hot temperature of the brine and  $T_y$  is the cold temperature of the brine. Figure 16 shows a graphical analysis of the pinch point calculations.

In Figure 15 the flow is counter current meaning that the hottest heat source vaporizes the working fluid while the cooler heat source preheats the working fluid. The abscissa is the percentage of the heat transferred, from the heat source to the working fluid, known as the heat demand. The heat supply is the geothermal mass flow line, but could be any heat source. The working fluid temperature increases until point 5 on Figure 15 where it starts to vaporize. Thereafter it remains at constant temperature until it is completely in the vapor phase. The difference in temperature between  $T_z$  and the temperature at point 5 is known as the pinch point temperature difference. As the pinch point temperature difference increases, the heat exchange becomes more efficient and requires a heat exchanger with a smaller surface area; however, not as much of the heat energy can be utilized. The opposite is also true; when the pinch point temperature difference is small, the heat exchange is less efficient, requiring a larger heat exchange

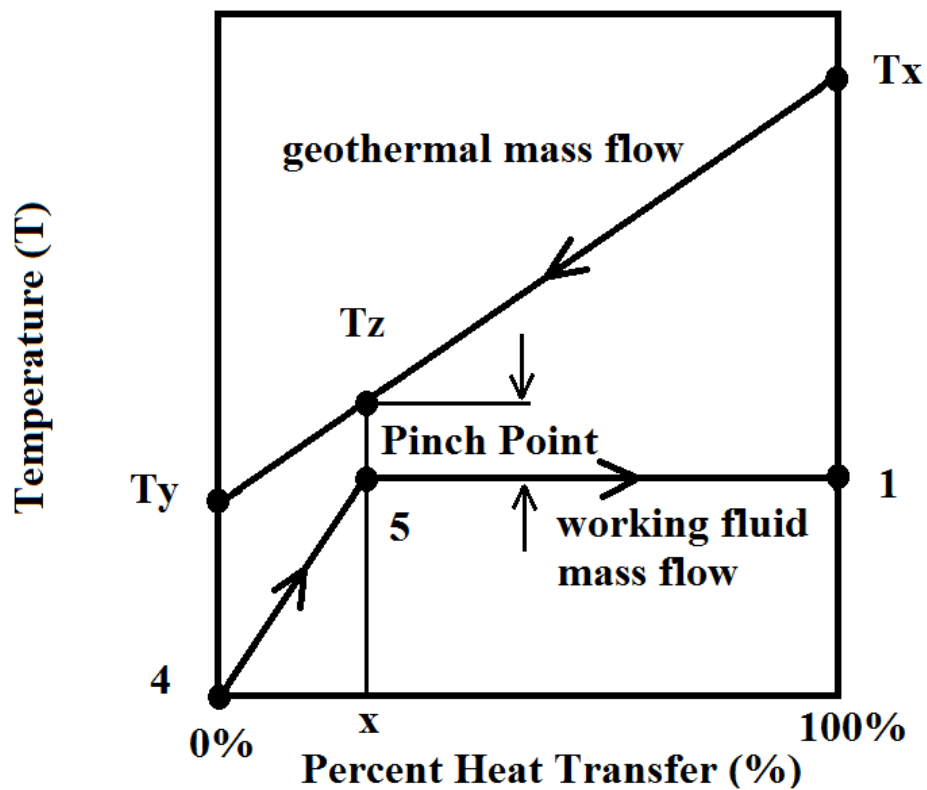


Figure 15 - T-q diagram for pinch point analysis.

surface area, although the utilization of the heat energy increases. An optimal pinch point temperature difference is determined by varying working fluids until one with desirable heat exchange properties is found which utilizes as much of the heat energy as possible.

### 3.3 Carnot and Triangular Cycles

The Carnot cycle is well known in thermodynamics as the maximum thermal efficiency of a power cycle that operates between a given temperature heat source and heat sink. The steps of the Carnot cycle are isentropic expansion, isothermal heat rejection, isentropic compression and isothermal heat addition. It has been proven in

various instances that the maximum thermal efficiency for a heat source and sink is given by Equation 13.

$$\eta_{carnot} = 1 - \frac{T_{cold}}{T_{hot}} \quad (13)$$

In this equation,  $\eta_{carnot}$  is the maximum efficiency a power cycle can operate at with a heat sink at temperature  $T_{cold}$  and a heat source at temperature  $T_{hot}$ . Both  $T_{cold}$  and  $T_{hot}$  must be expressed as absolute temperatures, Kelvin or Rankine. It is a misconception to believe that the maximum efficiency of a binary power plant is at Carnot efficiency. Since the heat source of the binary power plants cools as the heat energy is transferred into the working fluid the isothermal heat transfer step of the Carnot cycle does not exist. The maximum efficiency for a binary power plant is known as the trilateral or triangular efficiency. When the Carnot process is sketched on a temperature-entropy diagram it is rectangular in shape and the trilateral process is triangular. The steps in the trilateral cycle are as follows: isentropic expansion, isothermal heat rejection and the simultaneous heating of the working fluid and cooling of the heat source. The efficiency of the trilateral cycle can be calculated by using Equation 14.

$$\eta_{trilateral} = \frac{T_{hot} - T_{cold}}{T_{hot} + T_{cold}} \quad (14)$$

In Equation 14  $\eta_{trilateral}$  is the trilateral efficiency between a heat source at temperature  $T_{hot}$  and a heat sink at temperature  $T_{cold}$ . Once again, the temperatures must be measured on an absolute scale (DiPippo, Ideal thermal efficiency for geothermal binary plants, 2007).

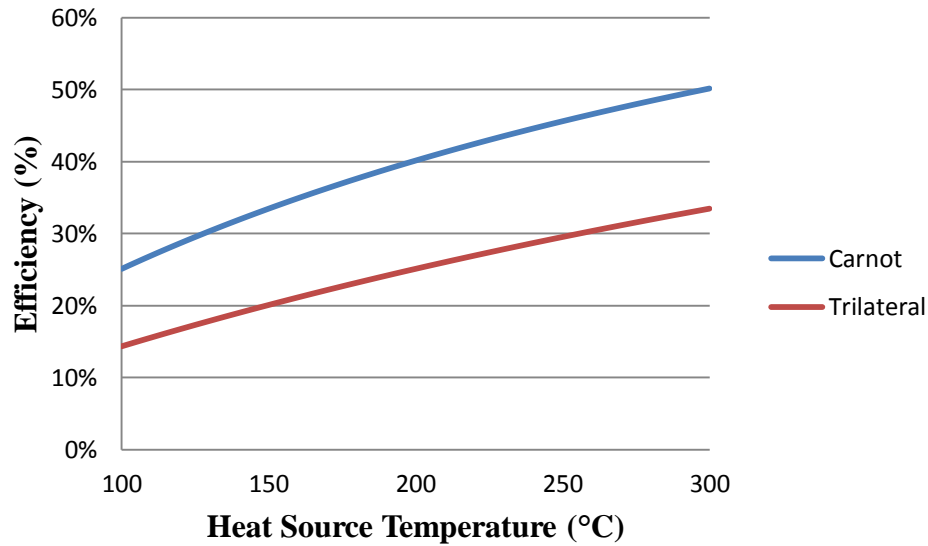


Figure 16 - Carnot and trilateral efficiency.

A comparison of the two cycles can be made to confirm that the trilateral cycle is less efficient than the Carnot cycle. Figure 16 depicts this. The heat sink is at a temperature of 25°C (77°F) and the heat source temperature ranges from 100-300°C (212-572°F). Since the trilateral cycle does not have the same steps as the Carnot cycle, it will have a lower efficiency. For example, with a heat sink at a temperature of 25°C (77°F) and a heat source of 200°C (392°F) the Carnot efficiency is 40.1% while the trilateral efficiency is 25.1%.

### 3.4 Thermal and Exergetic Efficiency

When discussing efficiency it is common for many to think of thermal efficiency based on the first law of thermodynamics. In its most basic definition thermal efficiency is the ratio of what is put into a system to what is produced from the system. In binary power plants, heat energy is put in and electrical power is produced. The thermal

efficiency of a binary power plant can be calculated by Equation 15 and can be combined with Equations 4 and 10 to incorporate the enthalpy of the working fluid.

$$\eta_{thermal} = \frac{W_{out}}{Q_{in}} = \frac{h_1 - h_2}{h_1 - h_4} \quad (15)$$

In this equation  $\eta_{thermal}$  is the thermal efficiency of the power cycle,  $W_{out}$  is the rate of electrical power produced and  $Q_{in}$  is the rate of heat added into the system. Binary power plants typically operate in the range of 8-14% thermal efficiency.

The next type of efficiency is based on the second law of thermodynamics and is called exergetic efficiency. The exergetic efficiency is sometimes called the utilization efficiency because it is a measure of how much work is produced in comparison to how much could potentially be produced. To calculate the exergetic efficiency of a power cycle one should use Equation 16.

$$\eta_{exergetic} = \frac{\dot{W}_{out}}{E} = \frac{\dot{W}_{out}}{\dot{m}[h_1 - h_0 - T_0(s_1 - s_0)]} \quad (16)$$

In this equation  $\eta_{exergetic}$  is the exergetic efficiency,  $\dot{W}_{out}$  is the rate of electrical energy produced, and  $E$  is the exergy of the process. Exergy is calculated by multiplying the mass flow rate of the working fluid,  $\dot{m}$ , by the difference of the enthalpy of the working fluid at the turbine inlet conditions,  $h_1$ , and the enthalpy of the working fluid at the dead state,  $h_0$ , and the product of the dead state temperature,  $T_0$ , with the difference of the entropy at the inlet of the turbine,  $s_1$  with the entropy of the working fluid at the dead

state conditions,  $s_0$  (DiPippo, Second Law assessment of binary plants generating power from low-temperature geothermal fluids, 2004). The dead state is the ambient temperature and pressure conditions which are the lowest possible conditions the working fluid could ever achieve which would produce the most amount of power. Using both of these definitions of efficiency will assist in the selection of the working fluid.

Each of these thermodynamic principles will assist in selecting a suitable working fluid for the geothermal-solar thermal power plant. The geothermal resource temperature and solar irradiance will also impact the selection of a working fluid. Chapter 4 will discuss geothermal and solar resource data in Newcastle, UT.



## **4. GEOTHERMAL AND SOLAR RESOURCE DATA**

Prior to making any engineering calculations on the design of a hybridized geothermal-solar thermal power plant, a resource evaluation must be done. The geothermal resource of the potential power plant in Newcastle, UT has been evaluated by others and some of the relevant information from technical articles will be presented. The solar resource had not been assessed; data were collected. The solar potential is summarized after an explanation of the types of solar irradiance and methods used to evaluate the raw solar data.

### **4.1 Geothermal Resource in Newcastle, UT**

The Newcastle geothermal resource is located in southern Utah, approximately 48 km (30 mi) west of Cedar City, Utah in the Escalante Valley on the northern slope of the Bull Valley Mountains. In 1975, relatively shallow irrigation wells were drilled and near boiling water came to the surface. At a depth of 91 m (300 ft), the water reached temperatures of 108°C (226°F) (Allred, 2004). Newcastle is known as a blind geothermal system because there are no surface manifestations such as hot springs or fumaroles in the nearby area. In the late 1970s and early 1980s various geologic studies were carried out to further understand the Newcastle geothermal system. It is believed that the system is recharged by deep circulating meteoric waters from within the Antelope Mountain Range. The circulating water is heated and intersects the Antelope fault zone at the base

of the mountain. The warm water ascends the fault zone and spills out into the alluvium filled valley. Figure 17 shows a conceptual model of this geothermal system

In addition to developing a conceptual model, temperature measurements were made to determine the heat flow in the area. Surface heat flow was calculated to be  $13.7 \text{ MW}_{\text{th}}$  which can be taken to represent a minimum natural heat flow (Chapman, 1981). At the present time, the primary use of the Newcastle geothermal system is to heat greenhouses owned by Milgro Nursery. This location is being studied in this thesis as a candidate location for hybrid solar-geothermal power generation.

Eleven temperature monitoring wells have been drilled and from 2001 to 2006 temperature measurements were made (Blackett, Newcastle, Utah Small-Scale Geothermal Power Development Project - Exploratory Drilling, 2004). Well MN-5 was

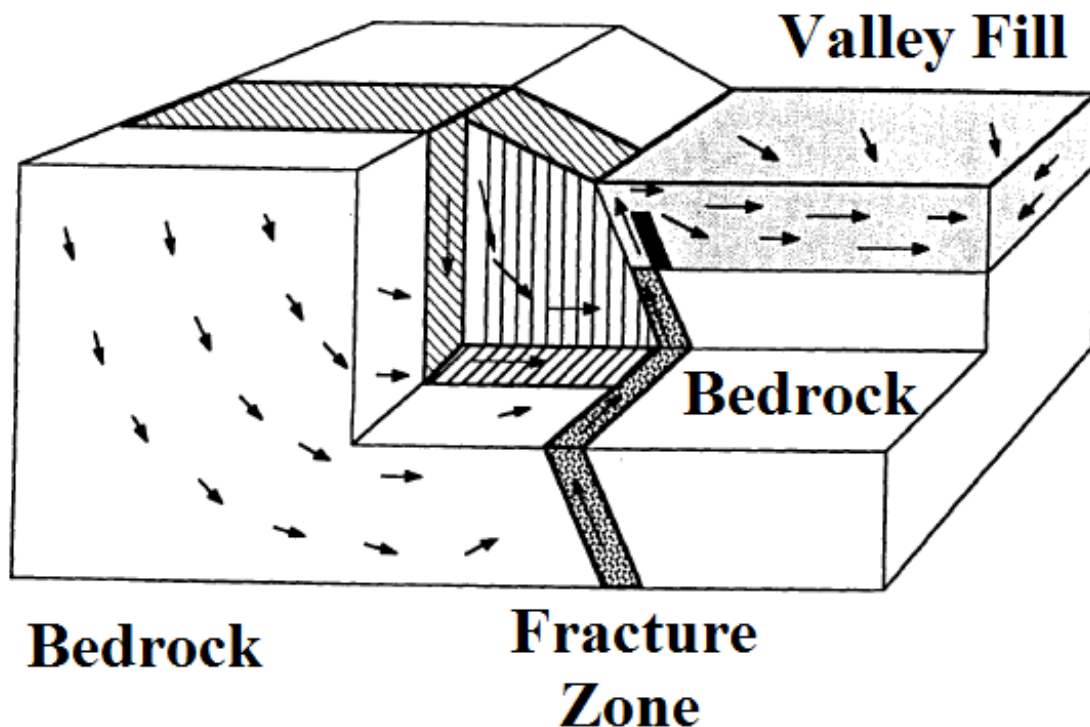


Figure 17 - Conceptual model of the Newcastle Geothermal System

going to be used for heating the Milgro greenhouses, but only reached a temperature of 102°C (215°F) when it was initially drilled in 1999. Since this well was drilled, measured temperatures were as high as 117.5°C (244°F). In well MN-6, the highest recorded temperature was 115°C (239°F); 117°C (243°F) in well MN-7. The measurements in each of these wells changed very little over the timeframe in which they were taken. From this and other nonpublic information, it is believed that the Newcastle geothermal system can produce fluid at 115.6°C (240°F) at a rate of 1,800 gallons per minute. See Appendix A for well maps, temperature-depth charts and heat flow map.

The Milgro owner's primary concern is to maintain the resource for use in heating the greenhouses and power production is seen as a secondary benefit. During the winter when there is the greatest demand for heating the greenhouses, water enters the greenhouses at nominally 82.2°C (180°F) and exits at 60°C (140°F) at a rate of 1,500 gallons per minute. Using an average density of 977 kg/m<sup>3</sup> and heat capacity of 4.19 kJ/kg·K, the heat demand of the greenhouses is determined to be 8.6 MW<sub>th</sub>. When the geothermal-solar thermal power plant is in operation, the rate will be higher at 1,800 gallons per minute, with a temperature drop in the geothermal water from 115.6°C (240°F) down to 65.5°C (150°F) within the power plant. Then, 8.6 MW<sub>th</sub> of heat will be extracted from the water to heat the greenhouse resulting in a reduction in temperature to 47°C (117°F). Operating in this manner, since the geothermal water will provide 23 MW<sub>th</sub> to the power cycle and 8.6 MW<sub>th</sub> to the greenhouses both the hybrid power plant and the greenhouses will function sustainably.

#### 4.2 Preliminary Solar Testing and Measurements

There are three different types of solar irradiance; Global Horizontal, Diffuse Horizontal and Direct Normal. Global Horizontal Irradiance (GHI) is the measure of the amount of irradiance that strikes a surface that is kept horizontal to the ground. Included in the GHI is the Diffuse Horizontal Irradiance (DHI) which is the irradiance that has been scattered by either clouds or particles in the atmosphere that reaches a surface that is horizontal to the ground. Direct Normal Irradiance (DNI) is the amount of irradiance that strikes a surface that is kept normal to the sun. Figure 18 illustrates each type of irradiance.

Notice that in Figure 18a there are two solar angles: the solar altitude angle and the zenith angle. The altitude angle is a measure of how many degrees the sun is positioned in the sky above the horizon and the zenith angle is a measure of how far the sun is down from a vector normal to the surface of the Earth. A pyranometer is used to measure both GHI and DHI; however, with the DHI measurement is made by a pyrhelimeter and a sun tracking device. Since the most expensive piece of equipment in measuring all of the types of solar irradiance is the sun tracking device used in the measurement of the DNI, it

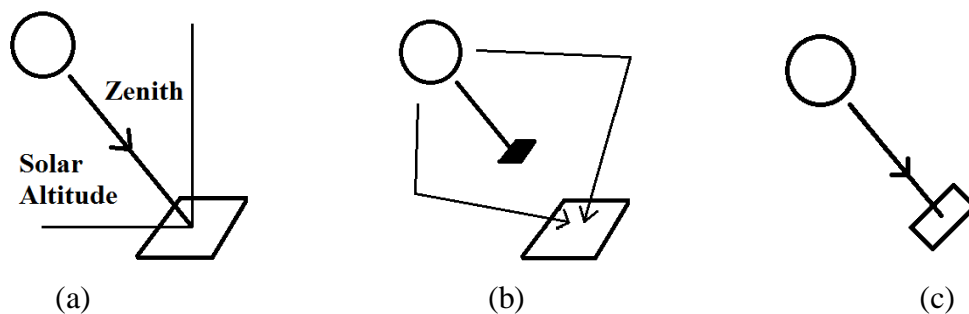


Figure 18 - Depiction of GHI (a), DHI (b) and DNI (c).

was decided that the GHI and DHI would be measured and the DNI would be calculated.

Equation 17 shows the relationship between the three types of radiation.

$$\text{DNI} \cdot \cos(Z) = \text{GHI} - \text{DHI} \quad (17)$$

In this equation DNI, GHI and DHI are the above mentioned types of irradiance and Z is the zenith angle, which is the angle measured between a vector normal to the surface of the earth and the vector which connects the Earth's surface and the sun. When the sun is rising or setting, the zenith angle is 90 degrees.

The equipment used to measure the GHI and DHI included two pyranometers, a shadow-band, computer with Labview software, a data acquisition system and a solar station. The 240-8101 Star Pyranometer was selected since it can measure irradiance ranging from 0 to 1,500 W/m<sup>2</sup>, operates over a temperature range from -40°C-60°C (-40°F-140°F) and has a fast response time. There are two versions of the 240-8101 Star Pyranometer, one with an amperage output and one with a voltage output. Since the amperage output also requires a power supply to generate the electric signal, the voltage output pyranometer was selected for measurements in this research program. A model 240-152 Shadow Band was purchased to block the direct irradiance from the pyranometer measuring the DHI. This shadow band can be used at latitudes up to 60° and can have a declination angle adjustment from -25° up to 25°. The declination angle is the measured angle between the plane made by the Earth's equator and the direct rays from the sun, thus its maximum and minimum are ±23.5 degrees since this is the angle of tilt of the

Earth's axis. When properly adjusted, the sun will follow the path of the shadow band which then will cast a shadow on the pyranometer behind it, allowing for the DHI measurement to be made. A solar station was built of two by fours and plywood in order to secure the pyranometers, shadow band and to house some of the data acquisition hardware. Since the computer needed to be indoors close to a power supply, a WLS/ENET-9162 data acquisition card slot was selected since it has both Ethernet and wireless capabilities. The appropriate data acquisition card was used in accordance with the voltage signals produced. The data were collected and stored on a laptop computer. The enabling Labview software was programmed to collect the year, month, day, hour, minute, second, GHI, DHI, and temperature measured from a thermocouple. The program was set up to record data every minute of the day starting at 4:30 am until 8:30 pm with the daylight savings time function turned off.

When setting up the solar station to make the irradiance measurements, one of the most important parameters needing to be taken into account is the alignment of the station. It is necessary that the shadow band faces directly south. A compass reading was used to determine this direction. The magnetic declination needs to be accounted for; a magnetic compass is based on magnetic north and not true north. Magnetic north is where the Earth's magnetic field points vertically downwards and is most often not the same as true north. Figure 19 is a map showing the variance between magnetic north and true north. The compass measurements were adjusted by subtracting  $12^\circ$ , since this is the difference between magnetic north and true north at the locations where solar measurements were made. After accounting for the magnetic declination and the solar station is facing true south, a latitude adjustment must be made on the side of the shadow



Figure 19 - Magnetic declination of the United States

band and the solar declination angle must be set. Once both of those angles are set, the pyranometers are ready for operation. A platform was constructed on the side of the station that faces south for the pyranometer measuring the GHI. The pyranometer in the shade of the shadow band measures DHI. Since the solar declination angle is constantly changing, the shadow band declination angle setting must also be adjusted. Depending on the time of year, it was determined that the shadow band could be adjusted two or three times per week. The shadow band's shadow is wider than the sensor area that needs to be shaded. Close to the summer and winter solstices, the band would need to be adjusted twice per week, and closer to the spring and fall equinoxes the band would have to be adjusted three times per week.

Before taking measurements at the Newcastle, UT site, the solar station was tested in two different locations. The initial test run was made on the roof of the Energy and

Geoscience Institute (EGI) facility, in Salt Lake City (40.758587 North, 111.827586 West). Figure 20 shows this installation. The goals of this test run were to ensure proper functioning and adjustment of the shadow band, to guarantee that the wireless data transmission capability was functioning and to confirm that data acquisition was sufficient.

It was discovered that the instructions for setting up the shadow band were not easily understood. The most important adjustments that needed to be made on the shadow band are the latitude adjustment and the solar declination angle adjustment. Once these were both set, the height for the platform to which the pyranometer was secured needed to be lowered and rails on the shadow band needed to be adjusted to ensure that the shadow falls on the sensor. The greatest obstacle turned out to be unreliable wireless



Figure 20 - Solar station set up at EGI.



connectivity due to the poor transmission through the roof of the building. It was assumed that, in the future, when the transmission was through air only, a sufficient connection could be made – a poor assumption it turned out. The data acquisition rate could not be thoroughly tested since the transmission was not successful. After initial testing was done at the EGI building from June to July of 2011 a field test was conducted in Ticaboo, UT (37.676229 North 110.697405 West). Figure 21 shows the solar station set-up in Ticaboo. Testing at Ticaboo allowed opportunity to test the apparatus in field conditions. Notice that the pyranometer that is towards the right foreground of the photo is completely in sunlight and the one in the middle background is shaded by the shadow band. Further testing of the data acquisition system was done in Ticaboo. Data were collected from July to September of 2011. One of the first issues that needed to be



Figure 21 - Solar Station in Ticaboo, UT

remedied was connectivity between the data acquisition system and the computer. It was found that every two to two and a half days the computer would need to be rebooted. Assuming this was due to connectivity the data acquisition hardware was hardwired to the computer via Ethernet cable, towards the beginning of September, 2011. This did not rectify the problem. Although some data were collected, additional modifications were still required. The data were being acquired every second and stored once per minute. However, all of the data were being plotted, forcing the computer to store all of the data on its RAM. When the RAM was filled, the computer would simply crash, requiring a reboot. Once the computer was rebooted, it would run until the RAM was again filled. These plots were eliminated and replaced by a display of the current measurement only. After this change was made in the software information was collected for 4 days before the apparatus was moved back to EGI, where data were collected for another 10 days. Once all of these tests were complete, the solar station was deployed again this time to the Newcastle geothermal site.

#### 4.3 Solar Resource in Newcastle, UT

For a hybrid solar geothermal location, in addition to evaluating the geothermal resource, the solar resource must be evaluated. This quantifies the available solar energy for the power cycle and allows the solar field to be sized. The Direct Normal Irradiance increases very quickly at the beginning of the day so the solar field will be sized and designed with an irradiance level  $750 \text{ W/m}^2$ . The solar capacity will be calculated as the amount of time the irradiance levels are above the design irradiance level. From the solar measurements it is possible to simply calculate the time, over an entire year, where the

irradiance levels are above a certain design value in this case  $750 \text{ W/m}^2$ . This calculation was done in two ways. The first way was by visual inspection of the solar irradiance charts. This methodology facilitated the exclusion of brief intermittent cloud cover. During these brief periods there would not be much effect on the amount of energy supplied to the power system. The opposite is also true. When there are long periods where irradiance levels are below designed requirements, it will take time for the heat transfer fluid to be reheated.

Irradiance measurements were taken in Newcastle, UT starting in the middle of November 2011 (37.658429 North 113.571087 West). Figures 22 through 25 are plots of these measurements. Each plot is followed by a brief description of how the adequate irradiance time was estimated. The GHI and DHI were measured and the DNI calculated. Figure 22 shows a sunny day in Newcastle, UT. The global and diffuse measurements are nearly the same from 7:30 am until 8:15 am which makes the calculation of the direct irradiance slightly inaccurate. Recognizing this difficulty, visual inspection was assumed to indicate that irradiance levels reached  $750 \text{ W/m}^2$  at 8:00 am. From 10:30 am to 11:00 am, the global irradiance levels almost match the diffuse values. This was due to a telephone pole located to the south of the solar station. When doing a visual inspection, such consistent irregularities could be ignored. It also appears that there may have been some cloud cover at 12:30 pm which could also be ignored since the heat transfer fluid in the solar troughs would still be at the temperature required by the power system over this short period of time. This day was allocated seven and one half hours of time when irradiance levels were above  $750 \text{ W/m}^2$ .

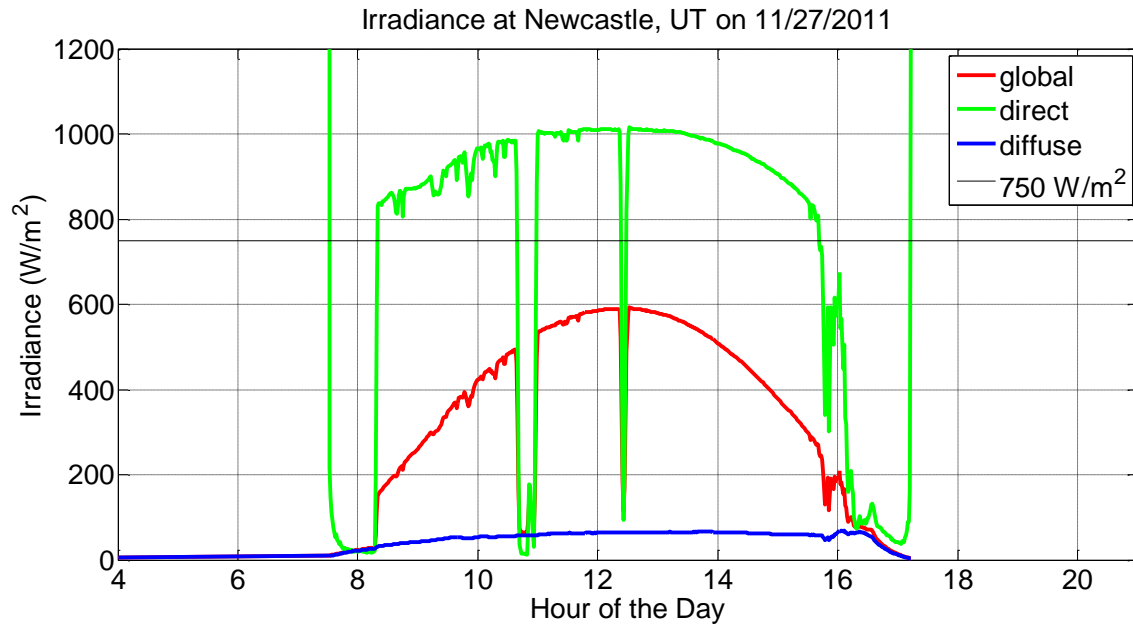


Figure 22 - Sunny day irradiance levels in Newcastle, UT.

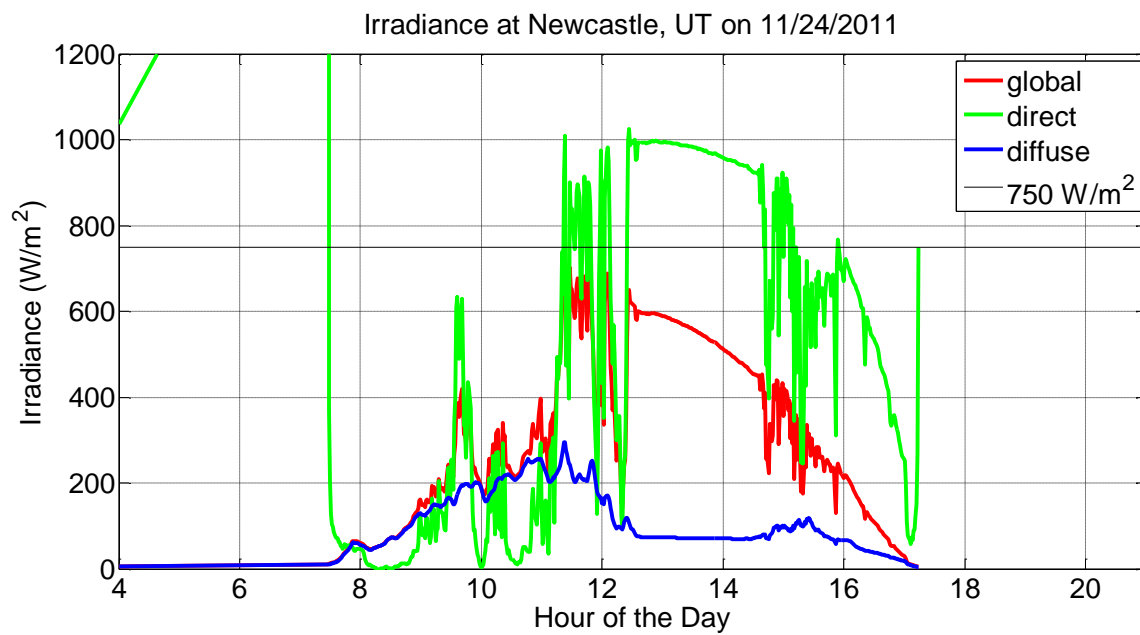


Figure 23 - Mostly cloudy day irradiance levels in Newcastle, UT.

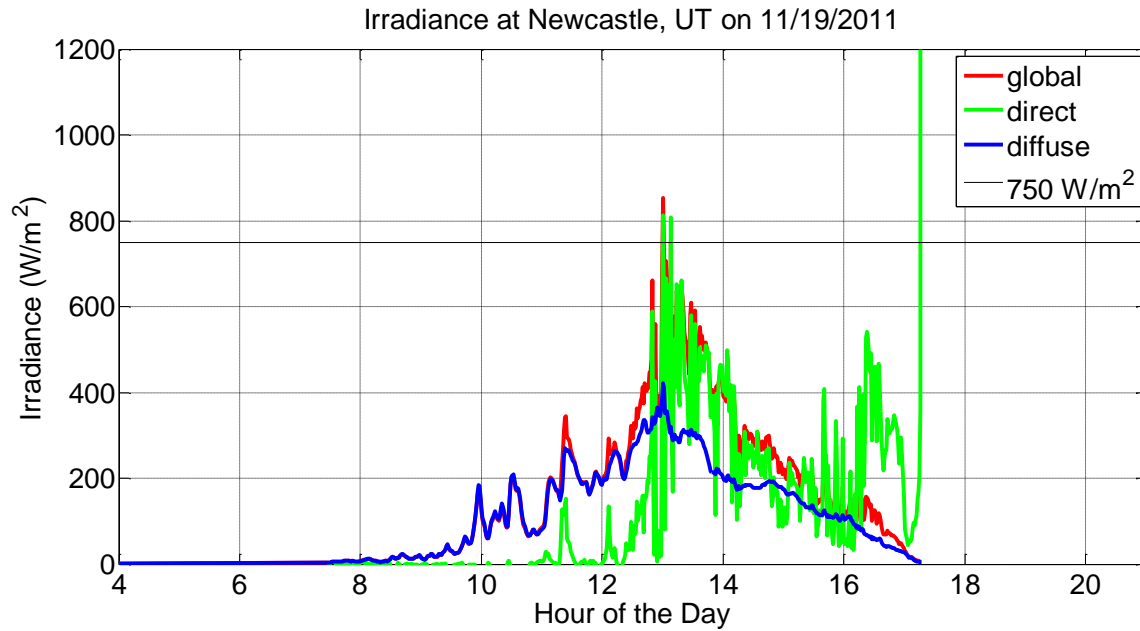


Figure 24 - Cloudy day irradiance levels in Newcastle, UT.

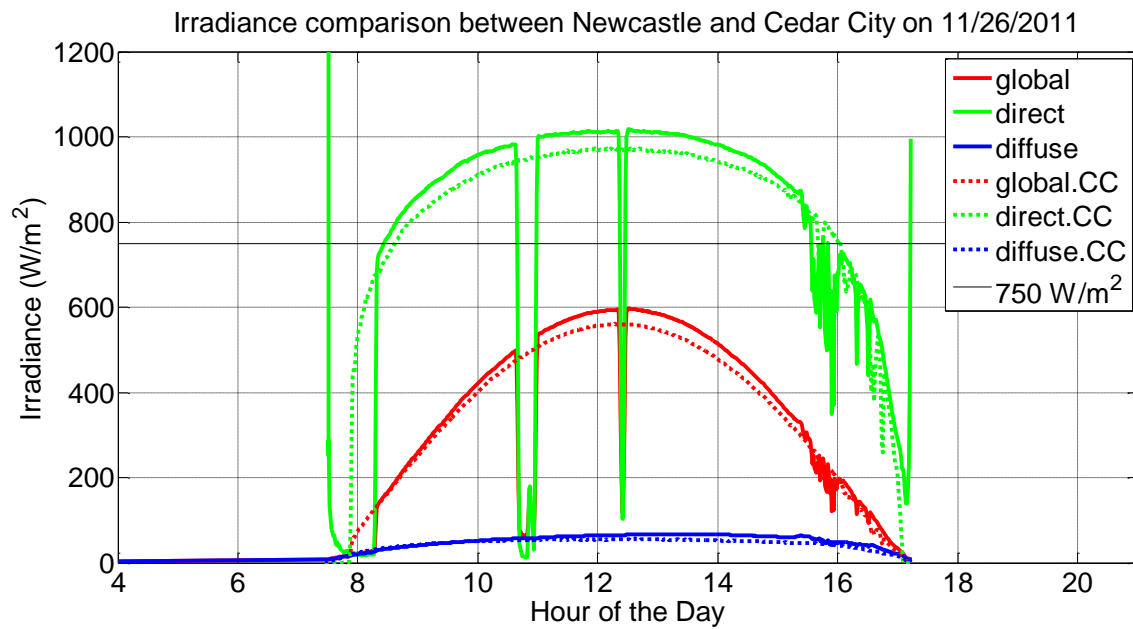


Figure 25 - Irradiance comparison between Newcastle and Cedar City on 11/26/2011.

The day shown in Figure 23 (November 24, 2011) is much different from that shown in Figure 22. During the first part November 24, 2011 (Figure 23) there was substantial cloud cover and the sun “came out” in the latter part of the day. From 8:00 am until 12:00 pm, the diffuse levels are much higher than from 12:00 pm until 5:00 pm meaning that more of the sun’s energy was scattered by the clouds during the morning. From 11:00 am until 12:00 pm there was a short amount of time when irradiance levels were above the design level, but at that time it is suggested not to produce by hybrid generation due to intermittent solar energy. Cloud cover also occurs starting at approximately 5:00 pm. November 24, 2011 was given a value of three hours above the design irradiance level. Figure 24 shows that it was cloudy all day. There would have been no sustained time interval above the design level of irradiance that would be useful to the power system.

Based on a 24-hour day, the irradiance levels would be over 750 W/m<sup>2</sup> in Newcastle, UT for the month of November 16.67% of the time (based on a 24-hour daily period). This is based on visual inspection of plots such as those shown in Figures 22 through 24. What would be most valuable is this same type of analysis would be data acquired over multiple years. As this was not possible for the specific Newcastle site, other options were explored. The National Renewable Energy Laboratory has a station that measures solar irradiance in Cedar City, UT (37.69601 N, 113.16483 W). This is approximately 30 miles east of Newcastle, UT. The Cedar City site has been recording solar irradiance levels since the summer of 2010. Figure 25 is a comparison of the data recorded at Newcastle and Cedar City on November 26, 2011.

From Figure 25 it is seen that the irradiance levels are almost identical in both locations. The same visual analysis was done on all of the irradiance data that have been recorded at Cedar City. The Cedar City site has data at one minute intervals from July 13, 2010 to the present time with a gap in the data from December 24, 2010 until February 1, 2011. No attempt to compensate for the missing data was made which could give an annual average slightly higher than may actually be. By visual inspection, over this entire time period, the DNI levels were above the design level 22.97%. A similar calculation for the data recorded at Newcastle yielded irradiance levels at or above the design level for roughly 23% of the year. When looking only at November 2011, visual inspection of the Cedar City data indicated adequate irradiance for 16.04% of the time based on a 24-hour day and Newcastle in November was 16.67%. This provided some degree of confidence that irradiance levels in Cedar City and Newcastle can be considered to be similar over the same period of time and that it could be assumed that Newcastle would be nominally the same. A second method, as described in the following paragraph, to evaluate the Cedar City data was by counting every minute that irradiance levels were above the design level. By this method the DNI was above the design level 24.11% of the time.

To this point, the discussion has been the design level of irradiance and how long it will be above a specific design point. Recall that the purpose of a hybrid geothermal-solar thermal power plant is to produce electricity at an increased efficiency since the power system has increased enthalpy from the solar energy. The “counting minutes” method of evaluating the solar resource is a more aggressive method because it assumes that when the instantaneous solar irradiance levels are above the design point, the heat transfer fluid instantaneously rises to the required temperature. It is known that heat

transfer takes a given amount of time which is why the “visual inspection” method is a more conservative and potentially more accurate method of evaluating the solar resource.

From measurements taken at Newcastle and Cedar City, UT it can be assumed that DNI levels will be above  $750 \text{ W/m}^2$  23% of the time based on a 24-hour day. Knowing this information will assist in the estimations of how much power could be produced on an annual basis. This in turn facilitates an estimation of the amount of electricity that could be generated from the hybrid facility. The following chapter will present more of the details on the design of the hybrid facility.



## 5. HYBRID GEOTHERMAL-SOLAR THERMAL POWER PLANT

In the previous chapters various discrete concepts have been discussed all of which have an impact on the design of geothermal-solar thermal power plants. This chapter will start to bring together the concepts that have been introduced and show their importance. Newcastle, UT will be used to demonstrate integration of the key concepts.

### 5.1 Design Considerations

The premise of a geothermal-solar thermal power plant is to have the geothermal portion of the power cycle running continuously; when adequate solar energy is available the operating conditions would change in order to produce more power at increased efficiency levels. Many different configurations of a hybrid plant such as this can be conceived. However what has been found that is the most efficient is often times the most simple. This has been the premise for the system proposed. Figure 26 is a schematic of a simple hybrid geothermal-solar thermal power plant. Notice that at the working fluid exit of the geo boiler / solar preheater the working fluid can go to either the solar boiler or to the low pressure turbine. During the night and/or when there is cloud cover such that the DNI is below  $750 \text{ W/m}^2$ , the working fluid would be pumped to a pressure so that it would be boiled by the geothermal fluid and a valve would close forcing the vapor to the low pressure turbine. When the sun is shining and the DNI is at or above  $750 \text{ W/m}^2$ , the working fluid would be pumped to a higher pressure, the valve to the low pressure

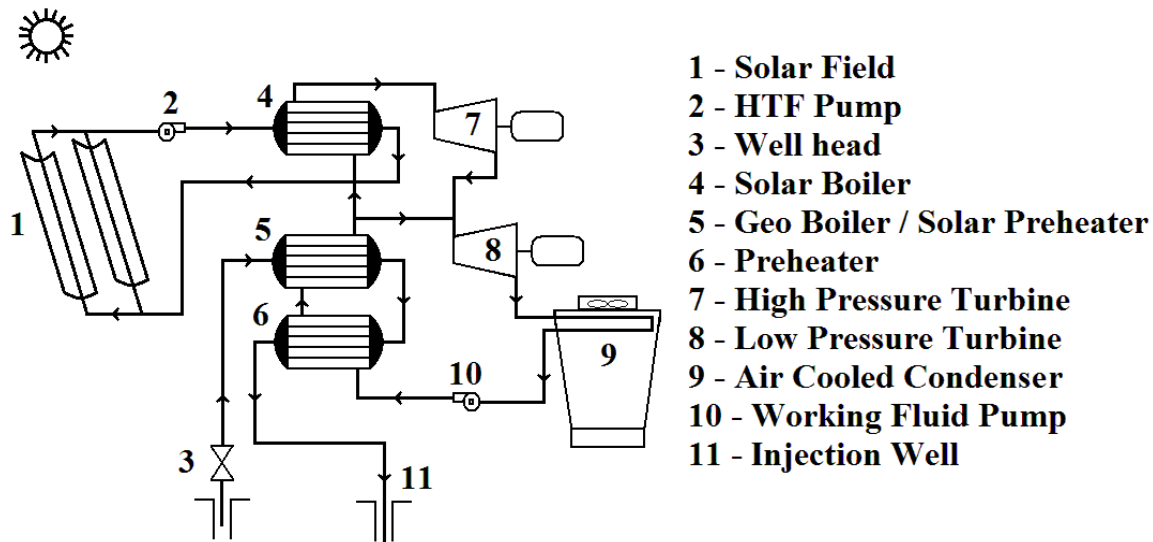


Figure 26 - Schematic of hybrid geothermal-solar thermal power plant.

turbine would close, the heat exchanger would become a preheater and the heat exchanger 4 would boil the working fluid by transferring heat from the solar heat transfer fluid to the working fluid. The working fluid would then go to the high pressure turbine. This turbine would be designed to extract energy so that the working fluids conditions would be similar to those at the exit of the geo boiler when operating at night or when there is cloud cover. It is most probable that heat exchanger 5 would have two exits, one for the vapor phase working fluid for night operation and one for liquid working fluid for day time operation.

Figure 27 is a P-h diagram of the process. During the night, the pump would pressurize the working fluid to the geo-only pressure, which would then be preheated and evaporated by the geothermal fluid. It would then be sent to the low pressure turbine, the exhaust would be condensed and the process would start again. During the day when the DNI is greater than  $750 \text{ W/m}^2$ , the pump would pressurize the fluid to the hybrid pressure, the geothermal fluid would preheat the working fluid and the fluid would be

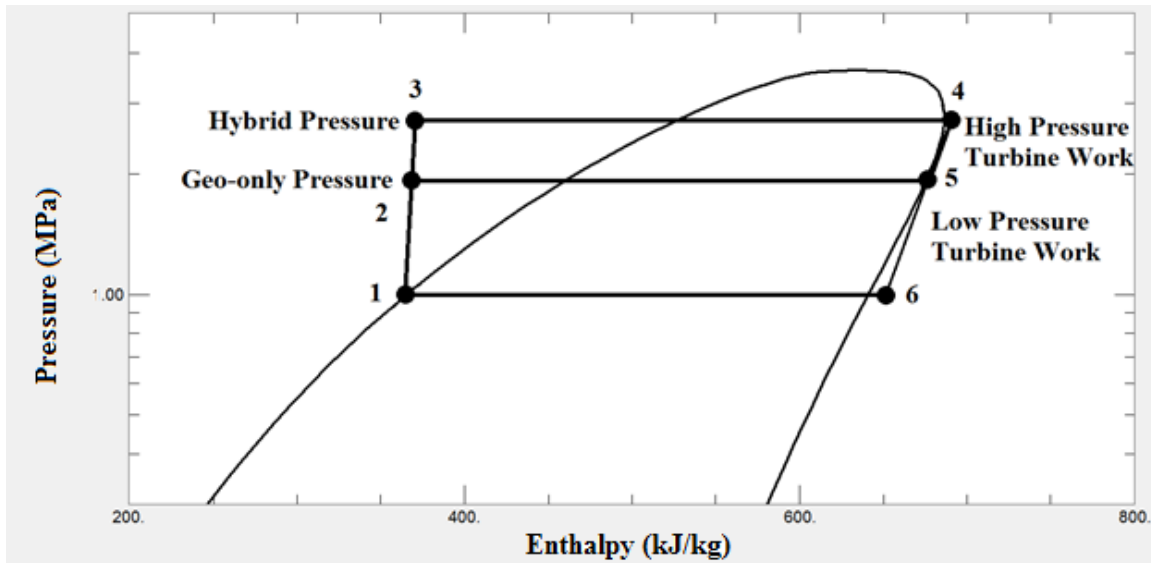


Figure 27 - P-h diagram of hybrid power plant.

boiled by the heat transfer fluid from the solar field. Then the high pressure vapor would go to the high pressure turbine, the exhaust of the high pressure turbine would go to the low pressure turbine, and finally the working fluid would be condensed and recycled.

The purpose of using the solar energy is to increase the enthalpy of the working fluid to its maximum. This could be done by super heating the vapor before it goes to the turbines. This is not advisable because the more a working fluid is super heated, the more super heat it will still have upon exiting the turbine. The reason for this can be seen in Figure 28. This figure shows a P-h diagram of isobutane with lines of constant entropy. An isentropic turbine has the same entropy at the inlet as the outlet, so if the inlet was super heated, the outlet would have roughly the same amount of super heat as in inlet. This would only create a greater cooling demand in the condenser.

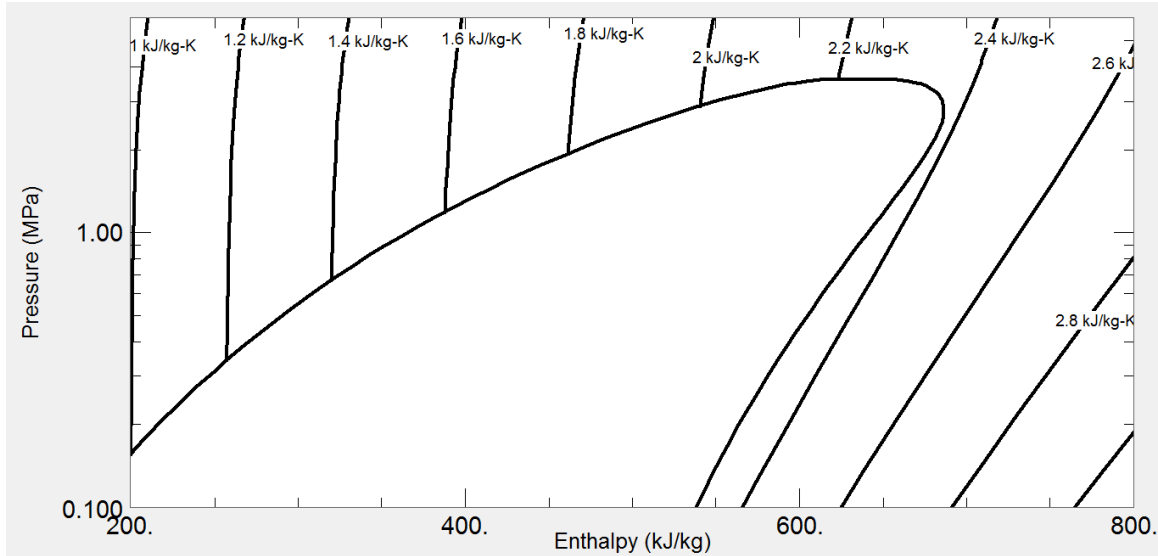


Figure 28 - P-h diagram of isobutane with lines of constant entropy.

### 5.2 Location and Minimizing the Footprint

The upper portion of Figure 29 shows the available geothermal and solar resources in the state of Utah. It can be seen that the Newcastle geothermal resource is one of the best locations to construct a geothermal-solar thermal power plant in the state of Utah. In this figure, the geothermal resources are outlined in green while the premium solar resources are the yellow, orange and red colors. For the solar measurements, the hotter the color means the area has a higher annual average DNI. The solar data are only plotted where the Earth has a low natural topographic gradient since solar power plants are easier to construct on regionally flatter surfaces. The lower portion of Figure 29 shows a magnified area south of the Escalante Valley and the blue star is Newcastle where both geothermal and solar resources are available. Minimizing the footprint of the hybrid power facility can be done in two ways; by constructing solar field immediately above the geothermal field and/or by increasing the thermal efficiency of the power system during daytime operation.

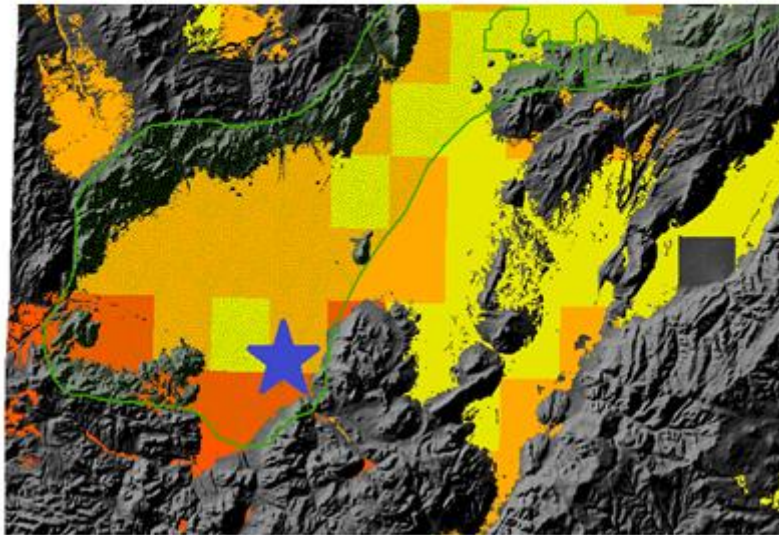
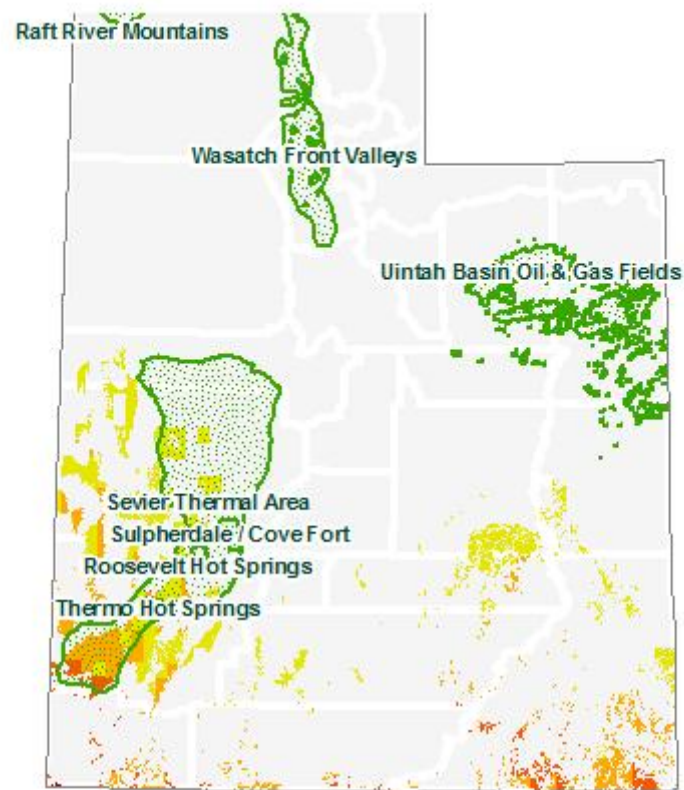


Figure 29 - Geothermal and solar resources in Utah. (Utah Renewable Energy Zone Interactive Map, 2012)

1. **Colocation:** Newcastle is in a remote area of Utah and there is much land that could be used near the geothermal wellheads where the solar field could be constructed. Using the geothermal field as part of the land where the solar field is constructed would reduce the overall footprint of the facility.
2. **Thermal Efficiency:** Increasing the thermal efficiency of the power cycle reduces the size of the solar field. For example, a small solar power plant produces 10 MW<sub>e</sub>. If this power plant produces at a thermal conversion rate of 9%, it would require 111 MW<sub>th</sub> of heat energy, whereas at 13% thermal efficiency it would only require 77 MW<sub>th</sub>. In other words, if this power facility increased its thermal efficiency by 4% it would require 34 MW<sub>th</sub> less thermal energy. At a design DNI of 750 W/m<sup>2</sup> this would reduce the size of the solar field by 65,120 m<sup>2</sup>. The area of the solar field assumes 70% field collection efficiency. The solar field is only 35% of the actual land area; this reduction in the size of the solar field would reduce the land area required by 46 acres.

### 5.3 Thermal Storage

Thermal storage was briefly mentioned in previous chapters when speaking of the solar power towers. It is also possible to implement thermal storage with solar trough plants. One way that this is done by heating the heat transfer fluid to 371°C (700°F) and transferring this thermal energy to cold salt and then storing the hot salt (Herrmann, 2004). For this hybrid geothermal-solar thermal power plant, salt thermal storage was not considered. It could be added in the future by increasing the size of the solar field to increase the amount of thermal energy collected. Even though solar salt was not

considered, there is still some thermal storage available in the heat transfer fluid. Throughout this thesis, the design level of  $750 \text{ W/m}^2$  was mentioned multiple times, but at peak hours of daylight hours, the DNI can be as high as  $1,000 \text{ W/m}^2$ . This would increase the temperature of the heat transfer fluid. As long as the heat transfer fluid does not reach its flash point it would be appropriate to store some thermal energy in the heat capacity of the heat transfer fluid. This would allow for increased production when there is intermittent cloud cover and for a brief period of time after the sun sets, as long as the heat transfer fluid remains at or above the temperature required to evaporate the working fluid at its increased pressure.

#### 5.4 Selection of Working Fluid

Many criteria were previously indicated (Section 1.3) for selecting a working fluid for a binary power plant. These same criteria will be used in the selection of a working fluid for use in the Newcastle, UT hybrid geothermal-solar thermal power plant. The criteria are toxicity of the fluid, fluid stability at high temperature and pressure, the fluid's boiling point at varying pressures, the fluid's flash point, its specific heat, thermal conductivity and latent heat. The number for toxicity was calculated based on Material Data Safety Sheets (MSDS) for each working fluid. The categories which were taken into account were inhalation, eye irritant, skin irritant and ingestion safety. One mark was given for each category where there was a negative impact and the sum of those marks makes up the toxicity score. The flash point was also recorded based on the fluid's MSDS. The boiling point pressure, liquid thermal conductivity and latent heat were all calculated using the Refprop 9 program. The boiling point pressure was based on the

operating pressure of the evaporator. The liquid thermal conductivity was based on the saturated liquid thermal conductivity at the evaporator pressure. The latent heat was based on latent heat of each working fluid at the evaporator pressure. Based on these criteria, and knowing that some of the information for r-245fa was not available, each of the working fluids were suggested that further calculations be done so a decision could be made based on the solar field requirements. Table 2 shows the results of these working fluid selection criteria.

Table 2 - Working fluid selection criteria.

Working Fluid	toxicity	boiling point Pressure (MPa)	flash point (K)	liquid thermal conductivity (W/m·K)	latent heat (kJ/kg)
butane	4	0.96	213	0.0852	296.3
isobutane	4	1.41	190	0.0895	248.0
pentane	4	0.33	224	0.1103	322.3
isopentane	4	0.41	222	0.1068	301.5
neopentane	4	0.72	266	0.0920	250.9
r-134a	3	3.79	523	0.0803	52.4
r-245fa	no data	0.81	no data	0.0875	151.5



## 6. FEASIBILITY

### 6.1 Process Simulations

Both daytime and night scenarios for the hybrid geothermal-solar thermal power plant were set up in the Promax process simulator. This was done as a second method of performing the power cycle calculations to ensure accuracy of previous results. The process simulator allows complex calculations with many variables to be done quickly and accurately. For all scenarios it was assumed that:

- there were no pressure losses in the heat exchangers
- the working fluid left the evaporators as a saturated vapor
- the air cooled condenser had air available at 70°F (21.1°C)
- 80% polytropic efficiency in the turbines
- 85% efficiency in the pump

When the DNI is at or above 750 W/m<sup>2</sup>, the following assumptions were made:

- the working fluid was preheated by the geothermal brine to 220°F (104.4°C)
- the solar field operates at 70% efficiency (Padilla, 2011)
- the solar field is 35% of the total land area required (Manente, 2011)

With these assumptions the process simulation programs was set up in Promax. Figure 30 shows an outline of the simulated process for geothermal only scenario. In this scenario the “Brine In” stream was set at 1,800 gallons per minute with an inlet temperature of 240°F (115.6°C) and the “Brine Out” stream was set to 150°F (65.5°C). The inlet energy stream for the “Solar HX” heat exchanger was set to zero because at conditions below the

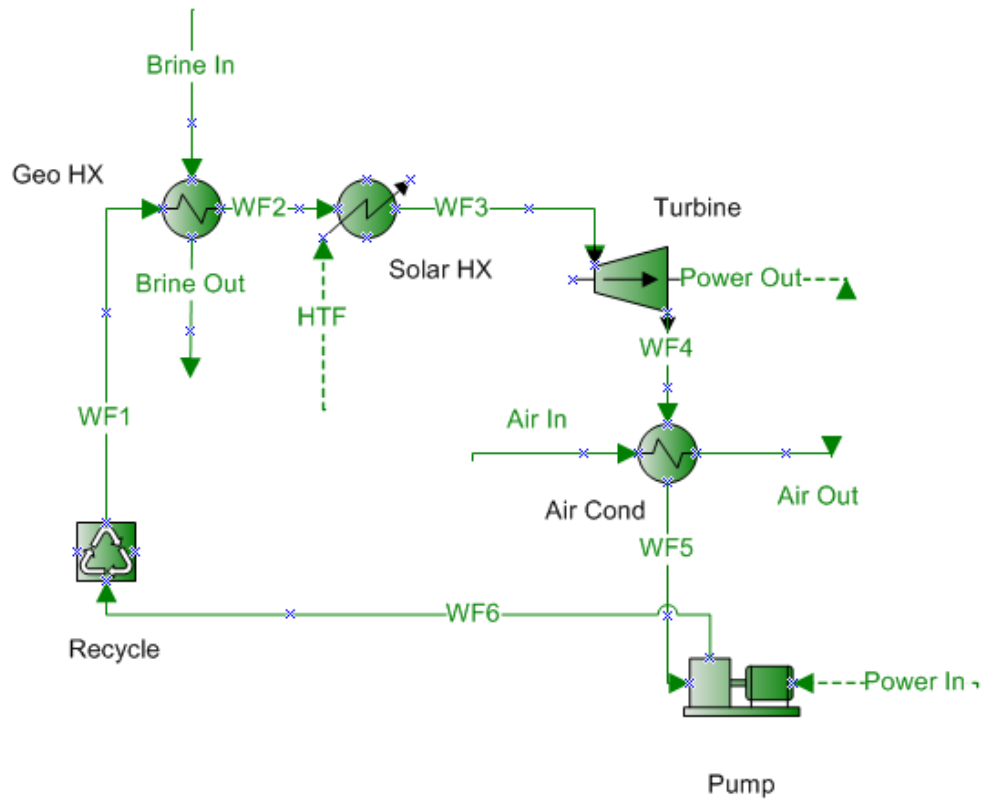


Figure 30 - Promax configuration of geothermal-only scenario.

design DNI level there will be no additional energy provided from the sun. The turbine outlet pressure was set so that the working fluid could be condensed by air that is heated from 70°F (21.1°C) up to 75°F (23.9°C). The pump was used to increase the working fluid's pressure after it has been condensed. The pump pressure needs to be sufficient so that the working fluid could still turn into a saturated vapor by the geothermal brine. The Promax calculations indicated that the geothermal brine alone could supply 22.4 MW<sub>th</sub> of energy to the power cycle. Table 3 shows operating conditions for various working fluids and Table 4 shows the associated power outputs. In Table 3 the fluid rate is the mass flow rate of the working fluid, pump outlet pressure of the working fluid from the pump and operating pressure of the evaporator, turbine outlet is the outlet pressure of the turbine

Table 3 - Results of Promax simulation for geothermal-only scenario.

Working Fluid	Fluid rate (kg/s)	Pump (psia)	Turbine outlet (psia)	Tevap (°F/°C)	Tcond (°F/°C)
butane	53.68	140	45	172.1 / 77.8	91.5 / 33.1
isobutane	55.56	205	50	180.5 / 82.5	76.0 / 24.4
pentane	50.8	48	11	168.5 / 75.8	82.1 / 27.8
isopentane	52.95	61	14	169.8 / 75.6	79.6 / 26.4
neopentane	59.76	104	28	173.8 / 78.8	83.8 / 28.8
r-134a	125.28	550	102	207.9 / 97.7	80.4 / 26.9
r-245fa	95.38	118	23	178.2 / 81.2	80.3 / 26.8

and operating pressure of the condenser, Tevap is the evaporator operating temperature and Tcond is the condenser operating temperature. In Table 4 Turbine is the power produced by the turbine, pump is the power consumed by the pump and  $\eta_{th}$  is the thermal efficiency of the cycle. Within the thermal efficiency calculations, the only parasitic load taken into account was the pump work. If an air cooled condenser is used, parasitic load from the fans should also be taken into account. Since no pressure drop was assumed, this pump pressure is also the evaporator's operating pressure. There may in fact be a slight pressure drop from the pump to the evaporator, but it will be minimal compared to the

Table 4 - Results of geo-only operation.

Working Fluid	Turbine (MWe)	Pump (MWe)	$\eta_{th}$
butane	2.02	0.07	8.71%
isobutane	2.46	0.13	10.40%
pentane	2.17	0.024	9.58%
isopentane	2.23	0.033	9.81%
neopentane	2.16	0.063	9.36%
r-134a	2.66	0.36	10.27%
r-245fa	2.31	0.055	10.07%

difference between the turbine exhaust and the pressure which must be produced by the pump. In an actual plant, a pressure gauge would communicate with the pump to maintain the pressure in the evaporator at the correct value. Table 4 shows that, depending on the working fluid, the power produced will range from 2.02-2.66 MWe and the thermal efficiency varies from 8.71%-10.40%.

When the DNI is above the  $750 \text{ W/m}^2$  design level, the geothermal-solar thermal hybridized plant will commence operation. This would require daily start up and shut down of the high pressure turbine. The geothermal brine still experiences a reduction in temperature from  $240^\circ\text{F}$  ( $115.6^\circ\text{C}$ ) to  $150^\circ\text{F}$  ( $65.5^\circ\text{C}$ ), but is now used to preheat the working fluid. After the working fluid is preheated by the geothermal brine to  $220^\circ\text{F}$  ( $104.4^\circ\text{C}$ ), it is evaporated by the heat transfer fluid from the solar field. In the hybrid scenario, the working pressure of the fluid was increased to the pressure which allowed for maximum enthalpy in the vapor phase and the flow rate was increased such that the geothermal brine preheated the working fluid to  $220^\circ\text{F}$  ( $104.4^\circ\text{C}$ ). Both of these criteria allowed for the most efficient operation of the hybrid facility. The maximum operating temperature of the heat transfer fluid needs to be kept in mind. A heat transfer fluid such as Therminol VP-1 has a maximum operating temperature of  $750^\circ\text{F}$  ( $398.9^\circ\text{C}$ ). This means that the evaporator operating temperature must be lower than the maximum operating temperature of the heat transfer fluid. After the working fluid is evaporated, it will pass through the high pressure turbine. The high pressure turbine will extract useful energy from the working fluid and its exhaust will be at the same pressure as the pressure of the geo-only turbine pressure inlet. By designing the plant in this manner the same turbine used in the geo-only scenario can be used as the low pressure turbine in the

hybrid scenario. The exhaust from the low pressure turbine will be cooled by air in the air-cooled condenser. Once the working fluid is back into the liquid phase, it will be pumped back to a higher pressure than in the geo-only scenario. The required pressure was selected by examination of the P-h diagrams of each working fluid. It was found that there is a pressure at which the enthalpy is maximized for the saturated vapor phase. This pressure was used as the pump pressure and the evaporator pressure. The flow rate of the working fluid was set by ensuring that the working fluid exited the “Geo HX” at 220°F (104.4°C). Figure 31 shows this hybrid process set up in the Promax process simulation software. Table 5 shows the operating conditions of the hybrid geothermal-solar thermal power. In Table 5 fluid rate is the mass flow rate of the working fluid, pump in the pressure of the working fluid after leaving the pump and operating pressure of the evaporator, HP turbine outlet and LP turbine outlet are the pressures of the exhaust of each turbine,  $T_{\text{evap}}$  is the operating temperature of the evaporator and  $T_{\text{cond}}$  is the operating temperature of the condenser.

Notice that in Table 5 all of the LP Turbine Outlet pressures are the same as the Turbine Outlet pressures of Table 3. These specific outlet pressures are required for each fluid to be condensed by the air. Similarly, the temperature in the condenser for the hybrid scenario shown in Table 5 is the same as in the geo-only scenario shown in Table 3. The evaporator temperatures are much higher than for the geo-only scenario. This is due to the increase in the working fluid pressure which requires a higher temperature to evaporate. Since all of the temperatures are still well under the maximum operating temperature of Therminol VP-1 heat transfer fluid it remains a possible choice in the

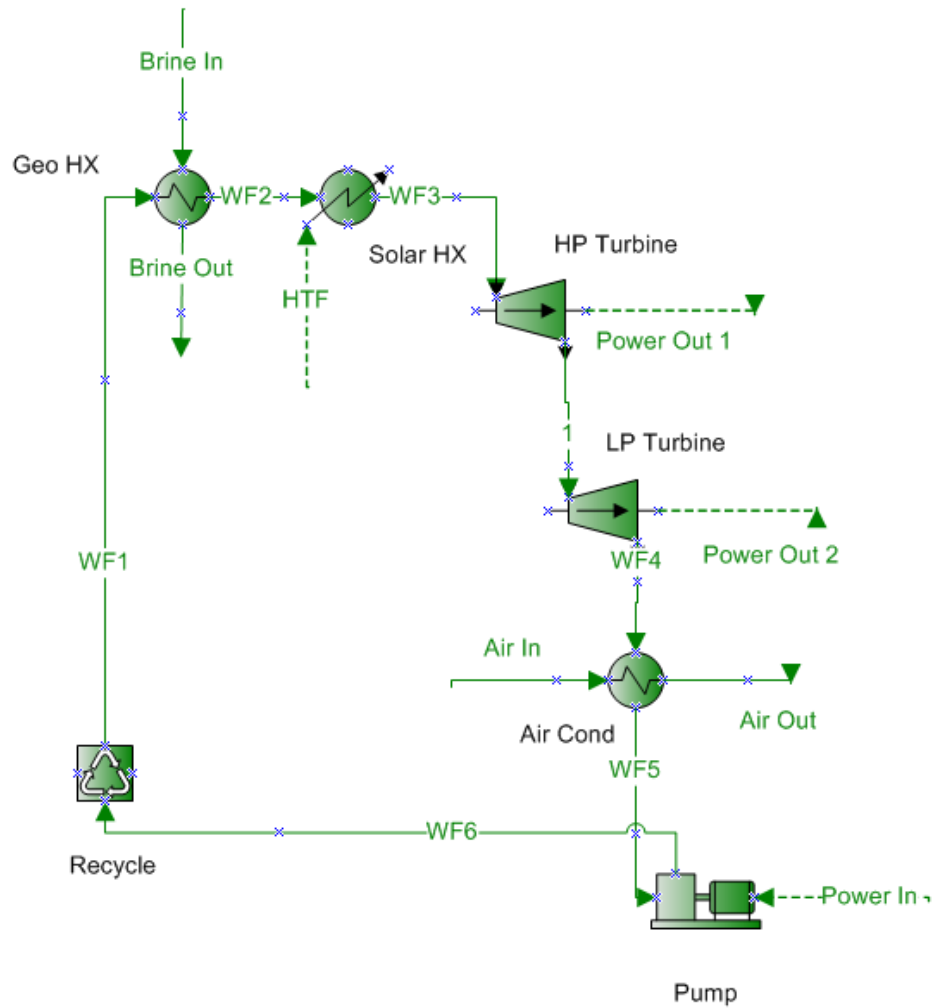


Figure 31- Promax configuration of geothermal-solar thermal hybrid scenario.

Table 5 - Operating conditions of the hybrid geothermal-solar thermal power plant.

Working Fluid	Fluid rate (kg/s)	Pump (psia)	HP Turbine Outlet (psia)	LP Turbine Outlet (psia)	Tevap (°F/°C)	Tcond (°F/°C)
butane	115.4	422	140	45	277 / 136	92 / 33
isobutane	101.2	406	205	50	247 / 120	76 / 24
pentane	119.1	402	48	11	363 / 184	82 / 28
isopentane	118.2	411	61	14	349 / 176	80 / 26
neopentane	118.6	390	104	28	302 / 150	84 / 29
r-134a	150	575	550	102	212 / 100	80 / 27
r-245fa	190.1	400	118	23	282 / 139	80 / 27

hybrid scenario. Table 6 shows the results of the operating conditions specified in Table 5.

The results summarized in Table 6 demonstrate that the increase in pressure in the working fluid is accompanied by an increase in thermal efficiency and an increase in power production. As previously explained, the increase in power production relates to the increase in the working fluid flow rate.

In order for the hybrid scenario to function, there is an energy requirement from the sun. The geothermal brine was only used to preheat the working fluid to 220°F (104.4°C) and the heat transfer fluid from the solar field would supply the remainder of the heat to preheat and evaporate the working fluid. Table 7 shows the amount of energy required to complete the preheat and evaporation, solar field size and total land size can be seen in Table 6.

The computations in Table 7 were based on a design DNI level of 750 W/m<sup>2</sup>, an energy collection efficiency of 70% for the solar field (Padilla, 2011) and the solar field is 35% of the land area (Manente, 2011).<sup>3</sup> It is easily seen that the greater the thermal energy requirement from the “Solar HX” the larger the land area required. With each

Table 6 - Results of hybrid geothermal-solar thermal operation.

Working Fluid	HP Turbine (MWe)	LP Turbine (MWe)	Total Power (MWe)	Pump (MWe)	η <sub>th</sub> (%)
butane	3.73	4.56	8.29	0.62	14.17
isobutane	1.87	4.58	6.45	0.53	13.69
pentane	6.81	5.87	12.68	0.61	17.39
isopentane	5.87	5.69	11.56	0.62	16.89
neopentane	3.75	4.72	8.47	0.6	14.61
r-134a	0.06	3.02	3.08	0.45	9.82
r-245fa	3.03	4.83	7.86	0.44	14.92

<sup>3</sup> The remaining area allow access to the panels for maintenance, cleaning and power block construction

Table 7 - Solar energy, solar field and land requirements.

Working Fluid	Solar HX (MWth)	Solar Field (m <sup>2</sup> )	Total Land (Acres)
butane	31.7	60,400	42.6
isobutane	20.8	39,695	28.0
pentane	47.0	89,524	63.2
isopentane	42.4	80,724	57.0
neopentane	31.5	59,943	42.3
r-134a	4.4	8,362	5.9
r-245fa	27.3	52,076	36.8

working fluid there was a different evaporator temperature. For each different evaporator temperature, the flow rate of the heat transfer fluid in the solar field would need to be adjusted. The total amount of energy collected depends on the size of the solar field while the temperature of the heat transfer fluid depends on the flow rate through the parabolic troughs.

Tables 8 and 9 are very important in deciding on which working fluid should be used. Table 8 shows how much power could be produced annually and the power to land ratio. Table 9 shows the annual power production and the thermal efficiency of both the geo-only and hybrid scenarios. Most of the working fluids considered would be suitable

Table 8 - Annual power production and land to power ratio.

Working Fluid	Geo-only (MWe)	Hybrid (MWe)	Annual Power (GWh/y)	Total Land (Acres)	Power/Land GWh/acre-y)
butane	2.02	8.29	28.8	42.6	0.68
isobutane	2.46	6.45	28.1	28.0	1.00
pentane	2.17	12.68	38.2	63.2	0.60
isopentane	2.23	11.56	36.4	57.0	0.64
neopentane	2.16	8.47	30.1	42.3	0.71
r-134a	2.66	3.08	22.9	5.9	3.89
r-245fa	2.31	7.86	29.8	36.8	0.81



Table 9 - Annual power and thermal efficiency.

Fluid	Annual Power (GWh/y)	Geo-only $\eta_{th}$ (%)	Hybrid $\eta_{th}$ (%)
butane	28.8	8.71%	14.17%
isobutane	28.1	10.40%	13.69%
pentane	38.2	9.58%	17.39%
isopentane	36.4	9.81%	16.89%
neopentane	30.1	9.36%	14.61%
r-134a	22.9	10.27%	9.82%
r-245fa	29.8	10.07%	14.92%

for use in the hybrid facility in Newcastle, UT. If land conservation is important, fluids with high power to land ratios should be selected and if power production is important, fluids with high thermal efficiencies should be selected.

## 6.2 Resulting Thermodynamics and Efficiency

Recall the previous discussion of a P-h diagram for binary cycle power plant evaluation (Section 3.2). These diagrams are also useful for some comparison and analysis of the geo-only and hybrid scenarios. Selection of a working fluid for the geothermal-solar thermal power plant implicitly should embody what will be called “room to grow.” This means that in the P-h diagram the geo-only scenario cannot operate near the working fluid’s critical pressure. An example of this is when isobutane is used as the working fluid. The P-h diagram in Figure 32 shows the geo-only scenario for isobutane with an operating pressure of 1.4 MPa (205 psia) and the critical pressure of isobutane is 3.63 MPa (526 psia). This provides the possibility for increasing the working fluid the working fluid’s pressure for the hybrid scenario.

The P-h diagram in Figure 32 was created with the assistance of Refprop 9 from the National Institute of Standards and Technology. A Microsoft Excel interface enables

use of this program to calculate thermodynamic data. Many working fluids can be interchanged quickly to obtain electric production rates, heating and cooling duties of the heat exchangers and parasitic loads from pumps. When selecting a working fluid, the q-T diagram must also be taken into account by doing a pinch point analysis (as described in section 3.2). This was also done in the Excel interface to Refprop program and the resulting q-T diagram is seen in Figure 33. The Promax process simulator also produces q-T diagram (Figure 34). The difference between these two q-T diagrams is that the calculation of energy transferred in Figure 33 was based on a percentage of the total heat transferred whereas, for the Promax simulations shown in Figure 34 the energy transferred was based on a measured amount of energy. Regardless, the important feature of the q-T diagram is that the heat supply and heat demand lines do not cross, and the heat demand line must always be below the heat supply line. If this were not the case, the heat energy would transfer in the reverse direction, meaning that the working fluid would be cooled instead of being heated by the geothermal brine.

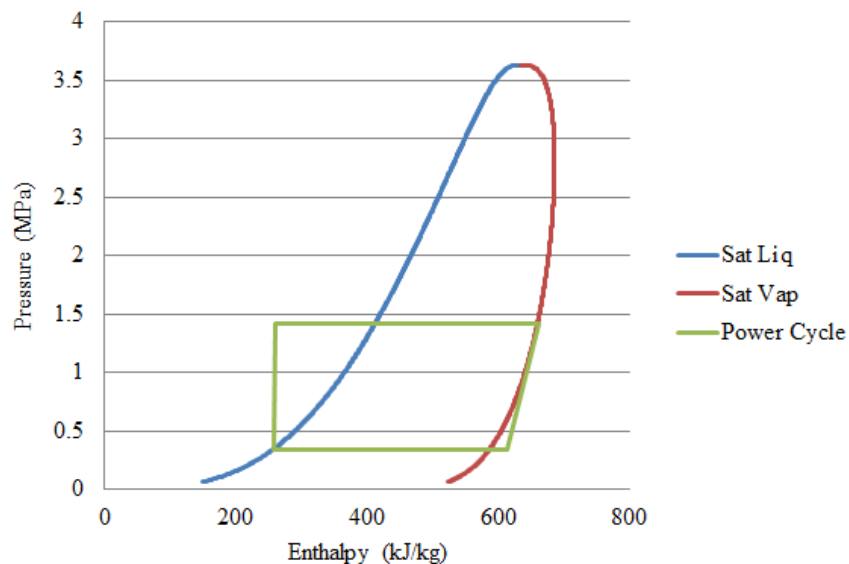


Figure 32 - P-h diagram of isobutane in geo-only scenario.

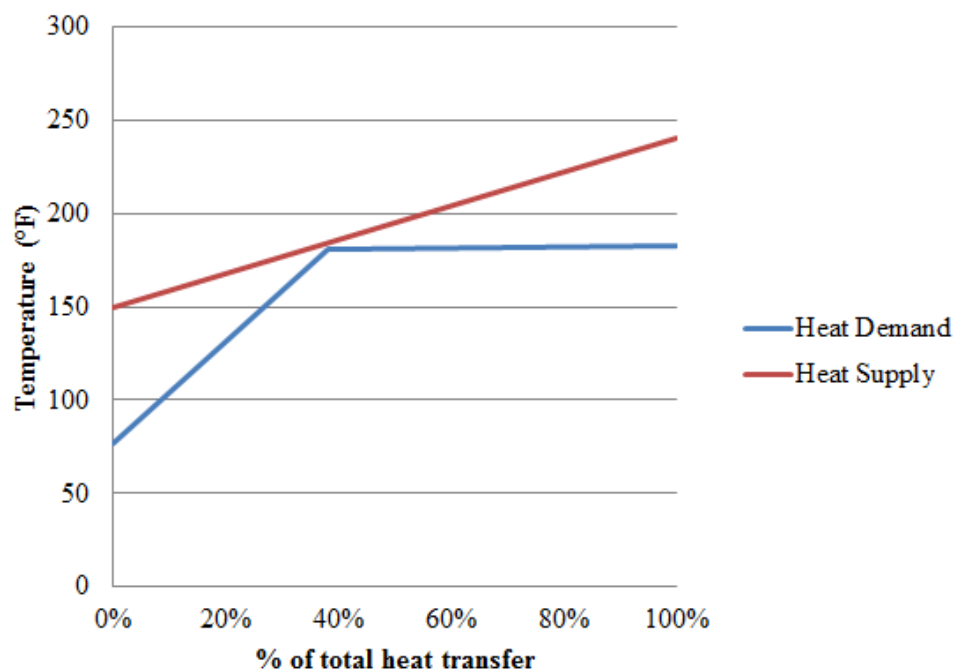


Figure 33 - q-T diagram for isobutane.

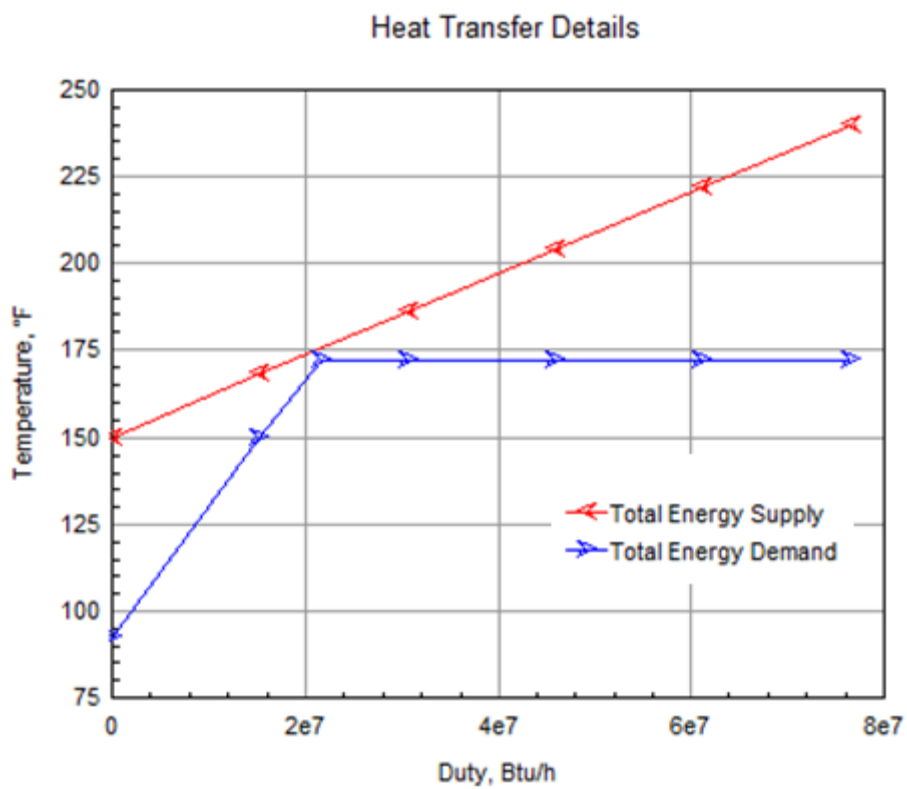


Figure 34 - Promax q-T diagram for isobutane.

In previous discussion of the P-h diagram there was minimal discussion on the meaning of “room to grow” in pressure. Figure 35 demonstrates the concept. This figure shows the operating pressure of the hybrid geothermal-solar thermal power plant. Comparing Figures 32 and 35 it is easily seen that the hybrid scenario operates at a higher pressure than the geo-only scenario. What is not shown is the intermediate thermodynamic state of the working fluid between the high pressure turbine and the low pressure turbine. Although the pathway from the inlet of the high pressure turbine to the exhaust of the low pressure turbine show as a linear process, crossing into the two phased envelope, the actual process may not be linear so there will be no condensation in the turbine.

Previously discussed were various criteria that should be used in the selection of the working fluid. One of these was that the working fluid should have a low latent heat, or energy required to change from the liquid to vapor phase at constant temperature.

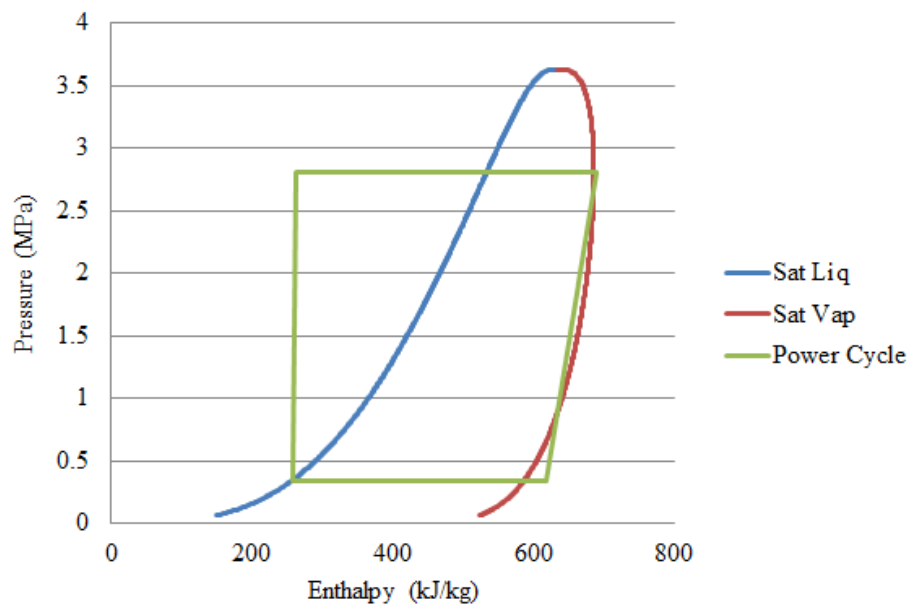


Figure 35 - P-h diagram of isobutane in the hybrid scenario.

Using Refprop, the latent heat of each working fluid at the evaporator's operating temperature was found. Table 10 summarizes these latent heats along with the thermal efficiency of the geo-only scenario. These data are also plotted in Figure 36.

From these data it is seen (Figure 36,  $R^2 = 0.32$ ) that there is a very weak linear correlation between the latent heat and the thermal efficiency. Isobutane, butane and neopentane do not follow the linear trend very well. There may be a stronger correlation between latent heat and thermal efficiency but to prove there is, more working fluids must be tested.

Table 10 - Latent heat and thermal efficiency.

Fluid	Latent Heat (kJ/kg)	$\eta_{th}$
butane	296.3	8.71%
isobutane	248.0	10.40%
pentane	322.3	9.58%
isopentane	301.5	9.81%
neopentane	250.9	9.36%
r-134a	52.4	10.27%
r-245fa	151.5	10.07%

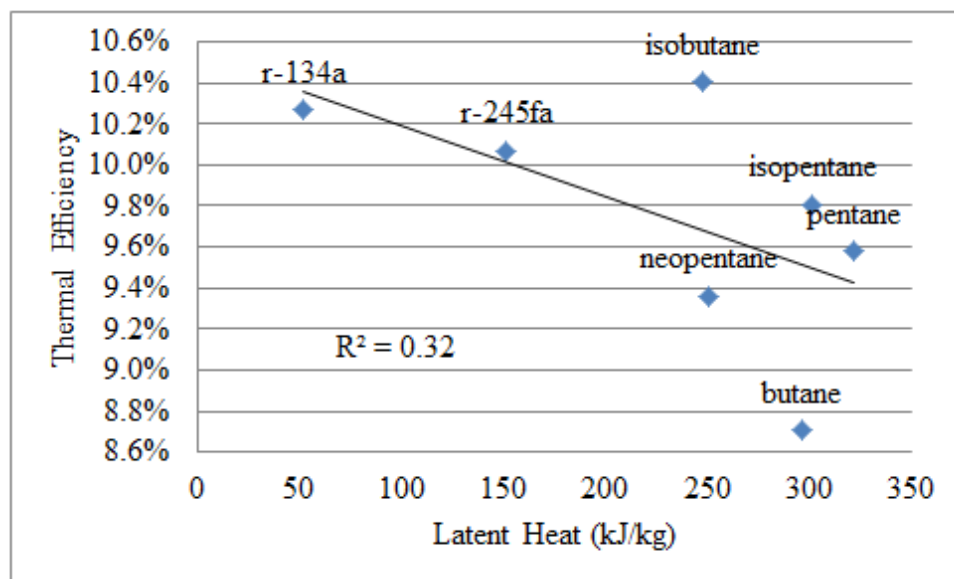


Figure 36 - Latent heat and thermal efficiency.

### 6.3 Recommendations for Newcastle Geothermal-Solar Thermal Hybrid Plant

The future of the geothermal-solar thermal hybrid power plant technology depends heavily on capital and operating costs including construction, materials, parabolic troughs, process equipment, working fluid, heat transfer fluid and plant maintenance. Capital cost could be depreciated by production and sale of electric power and by electric cost savings at the Milgro Newcastle greenhouses since the power will be consumed by that facility. Since the limited solar data taken at Newcastle, UT matched very well with NREL's Cedar City, UT data it was presumed that Cedar City information could be used to represent Newcastle DNI measurements throughout the year. It is recommended that solar irradiance measurements continue to be taken to compare with those acquired at Cedar City - until at least one year of measurements has been acquired. The same method of solar resource evaluation as described in section 4.3 should be followed.

Pending economic viability, a hybrid geothermal-solar thermal power facility Newcastle, UT would be the first facility of its kind. The rationale for selecting the optimal working fluid would be as follows.

- As shown in Table 7, r-134a had the largest power-to-land ratio. However, it is not recommended as the preferred working fluid. There is minimal "room to grow" in its power cycle on the P-h diagram. The geo-only operating pressure for r-134a is already near its critical pressure.
- Depending on the land available, 28 or 57 acres, where the solar field that can be constructed isobutane or isopentane are the recommended working fluids. Both of

these working fluids demonstrate an increase in thermal efficiency in their power cycles with the solar energy.

- The decision to select isobutene or isopentane depends on whether power production or reduced footprint is more important.
  - If it is desired to conserve land, choose isobutane,
  - If increased power production is desired, isopentane is recommended.

After the facility has been in operation for one to two years and lined out, its performance can be evaluated. While a test facility at Newcastle is in this proving period other low temperature geothermal systems could be sought out as future potential sites for hybrid power facilities.

## **APPENDIX A**

### **GEOHERMAL RESOURCE**

This appendix contains two maps for the well locations in Newcastle, UT (Figures A1 and A2) and temperature depth monitoring for select wells (Figures A3-A5). In Figure A1 wells NC-2 through NC-11 and CHR-1 were used as thermal gradient wells, wells NC-13 through NC-27 were additional thermal gradient drilled in a second phase of exploration, and wells WS-1, WS-4, WS-5 and WS-6 were drilled as irrigation wells and were used for fluid analysis. Figure A2 shows a map of the wells that were used to monitor the change in temperature over time. Figures A3-A5 show the results of this monitoring from 2001-2006 and show a maximum temperature of 115.6°C (240°F) (Blackett, Temperature-Depth Monitoring in the Newcastle Geothermal System, 2007). Figure A6 is the heat flow map which gives a heat anomaly of 13.7 MW<sub>th</sub>. This is considered to be a minimum of natural heat recharge (Chapman, 1981).



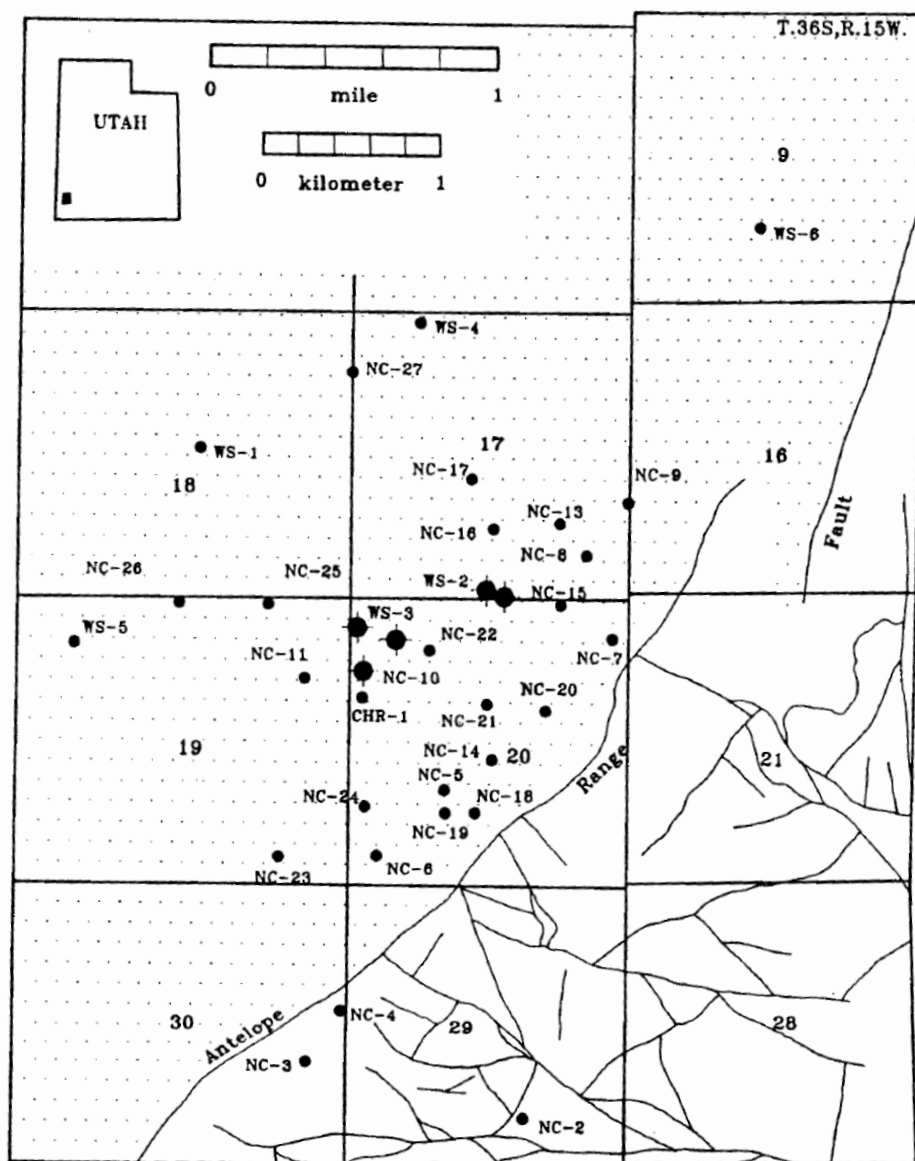


Figure A1 - Wells at Newcastle, UT

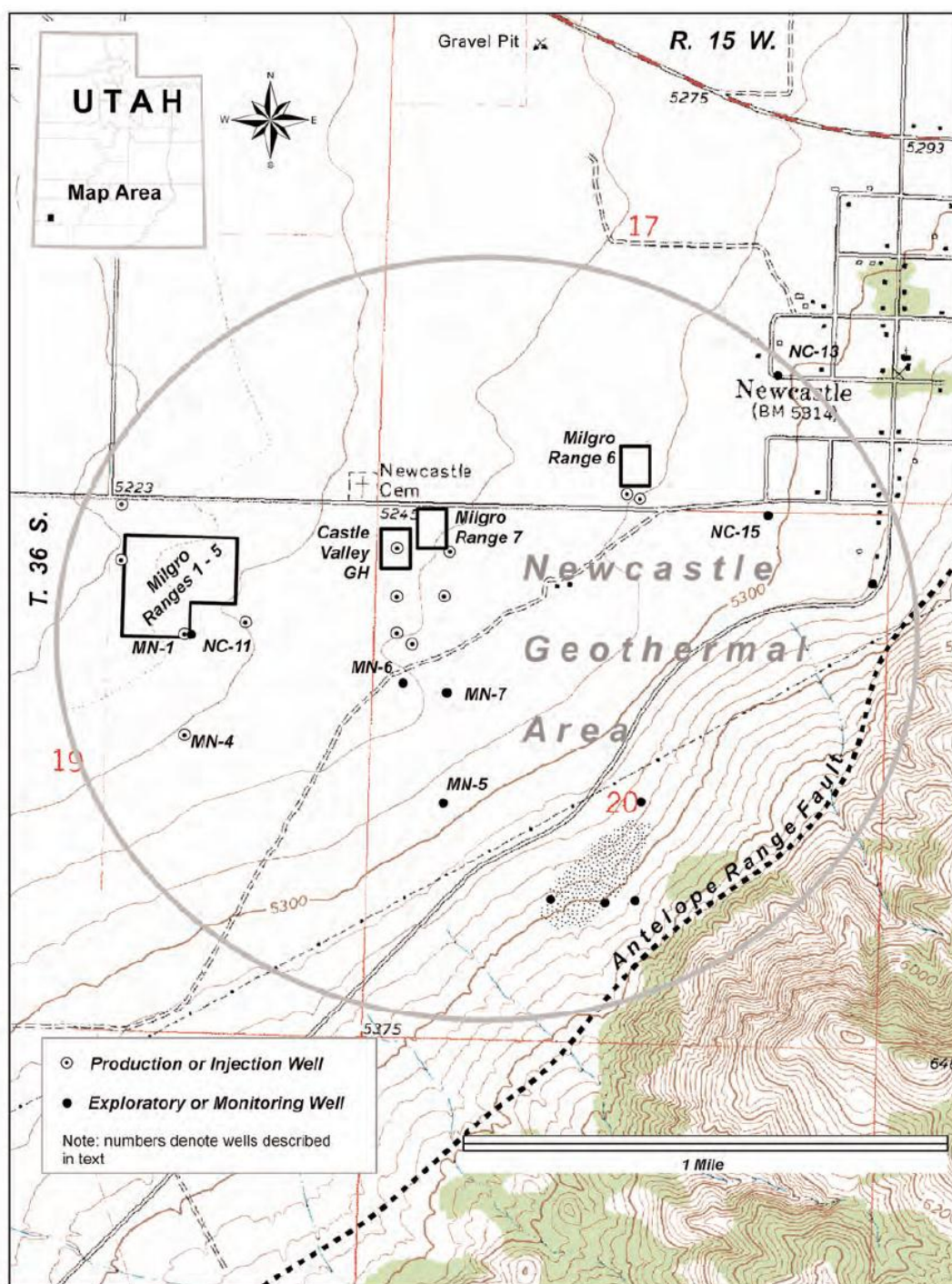


Figure A2 - More well locations at Newcastle, UT.

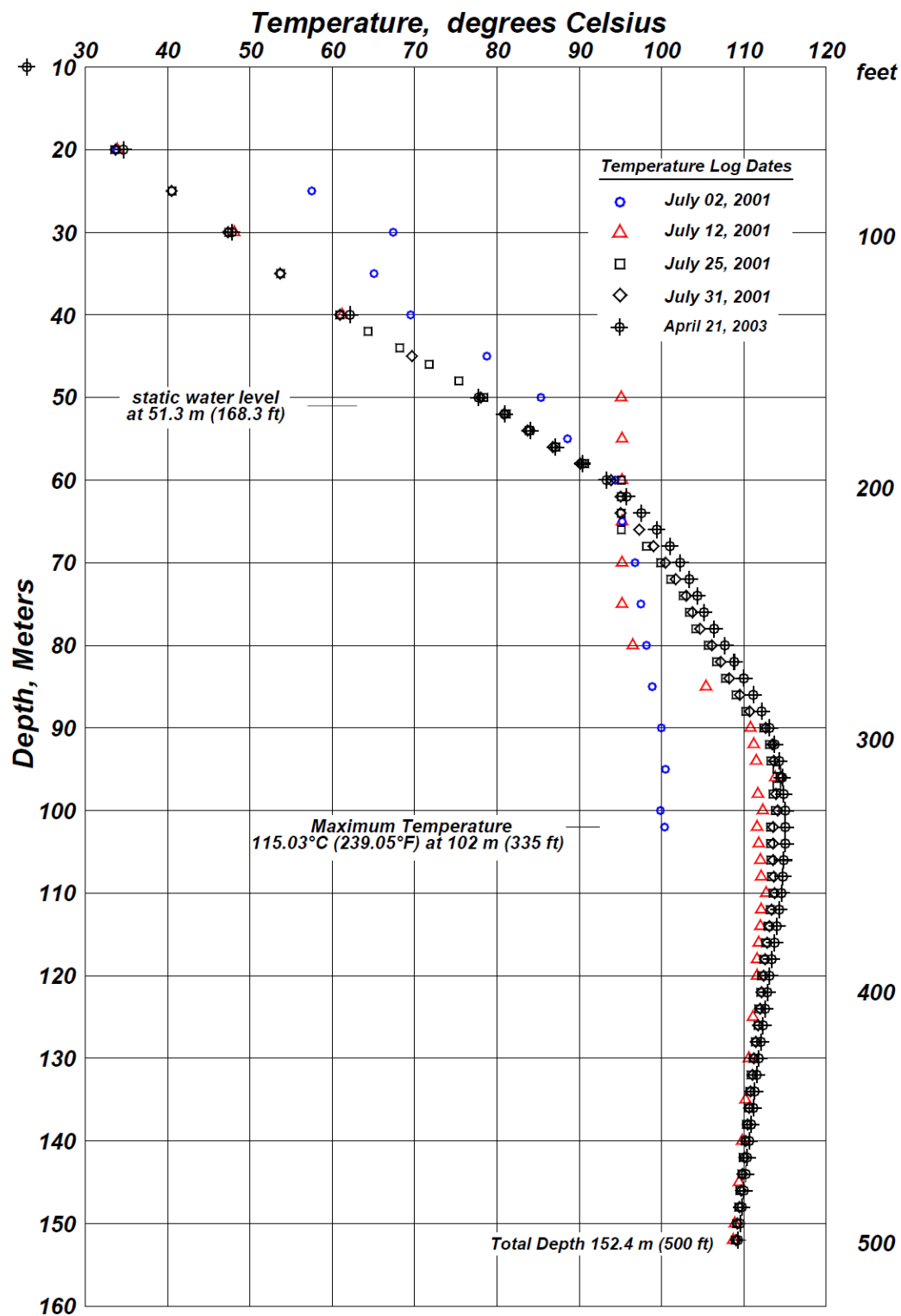


Figure A3 - Temperature-depth monitoring at well MN-6

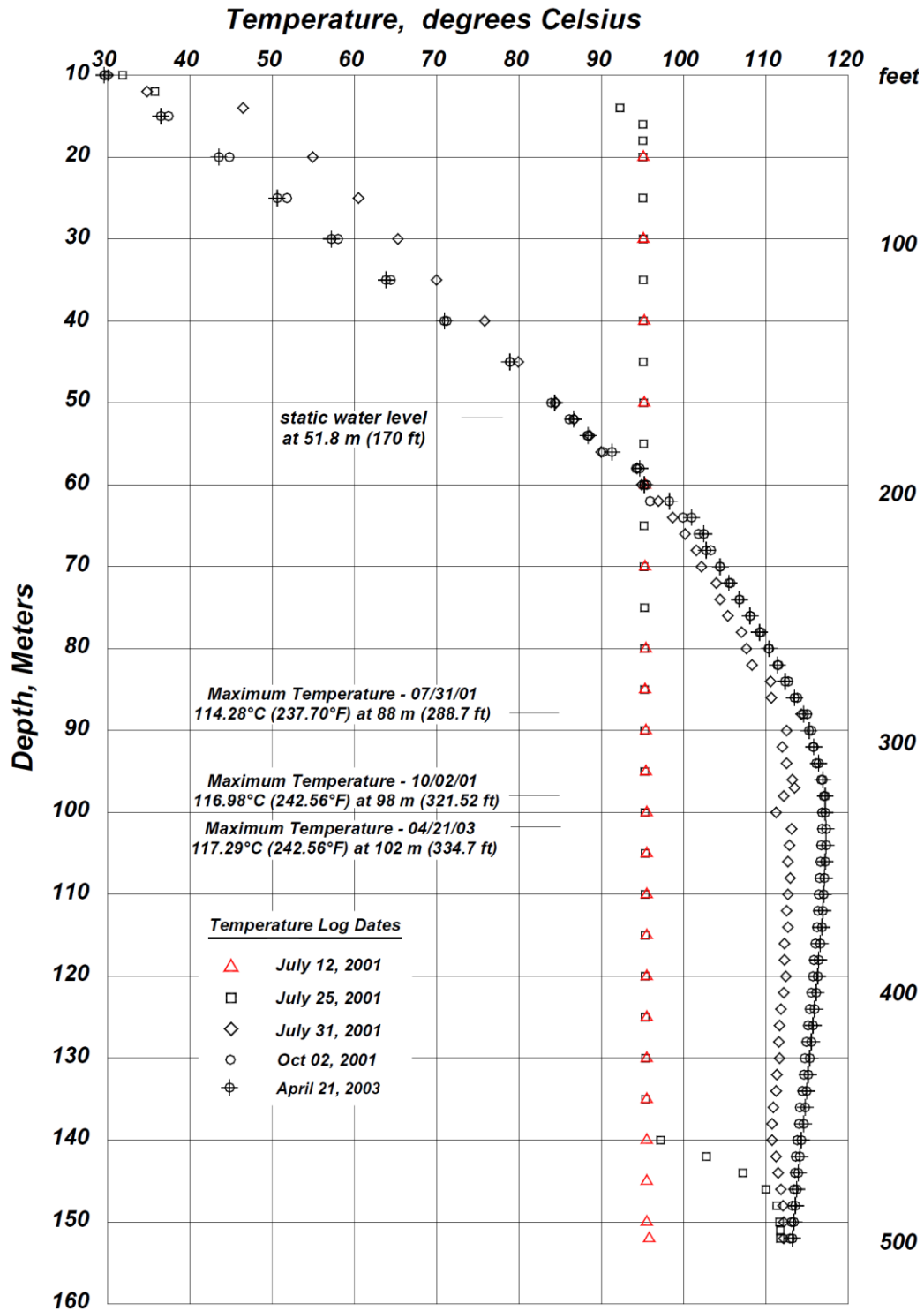


Figure A4 - Temperature-depth monitoring at well MN-7.

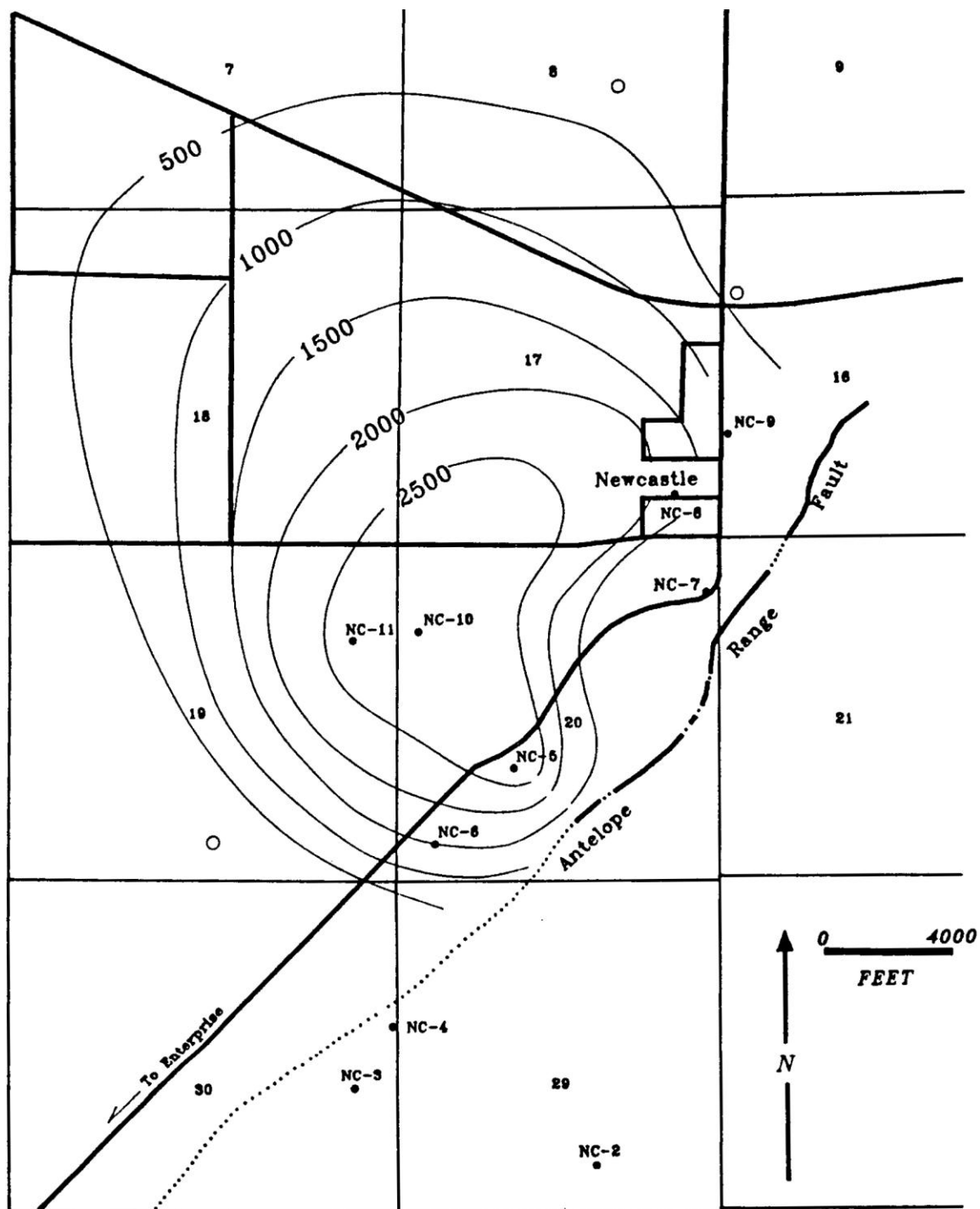


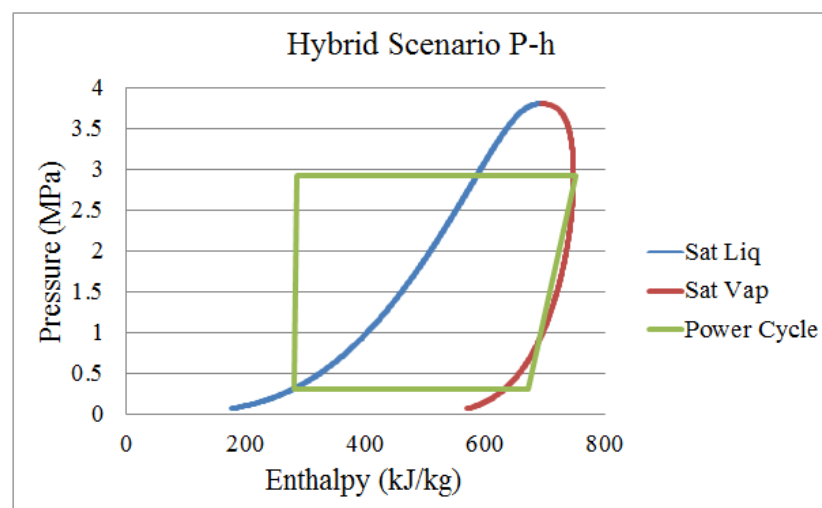
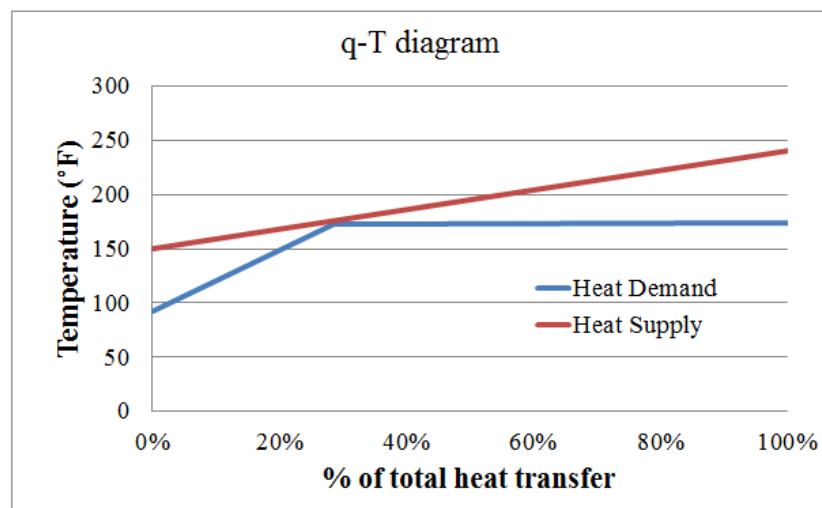
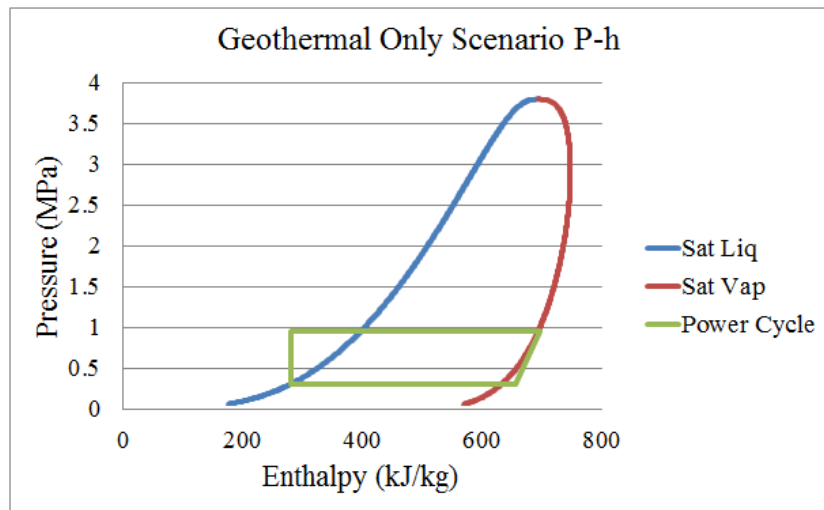
Figure A5 - Heat flow map of Newcastle, UT

## **APPENDIX B**

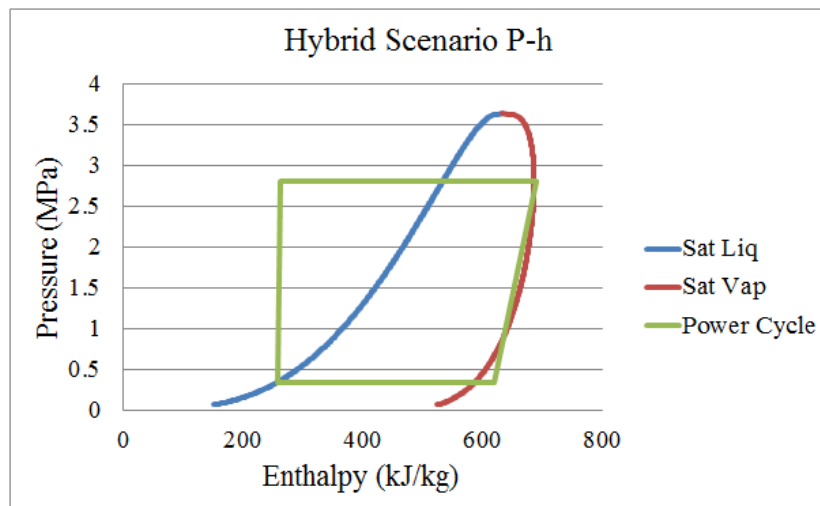
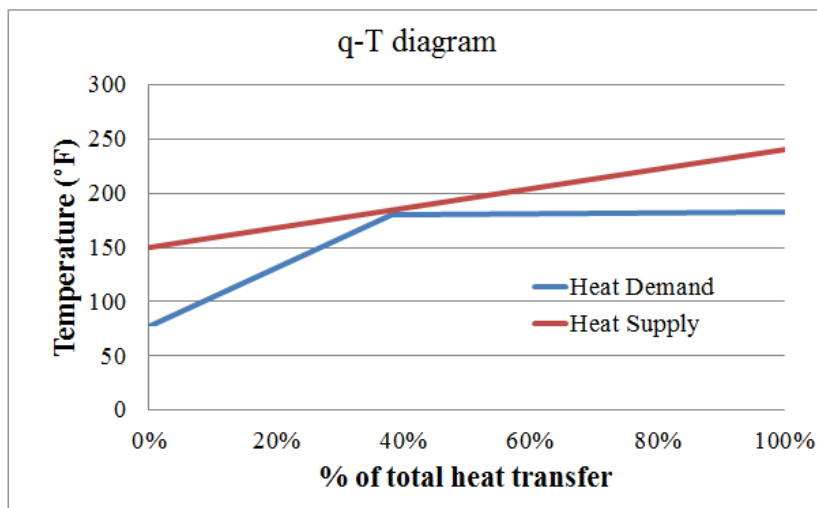
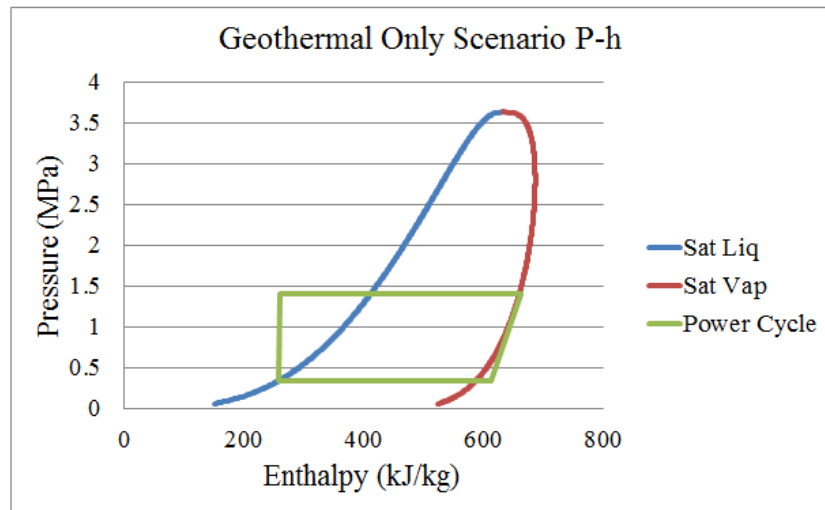
### **P-H AND Q-T DIAGRAMS**

This appendix contains the P-h diagrams for the geothermal only scenario, q-T for the geothermal only scenario and P-h for the hybrid scenario. In the P-h diagrams, the blue lines represent the saturated liquid phase, red lines represent the saturated vapor phase and the green lines represent the power cycle. In the q-T diagrams, the red line is the heat supply, the geothermal brine, and the blue line is the heat demand, the working fluid. The operating conditions were taken from the Promax simulation and entered into the Refprop 9 interface. The pinch point temperature in the Promax simulation was 5°F and varied to as low as 3.5°F in the Refprop excel interface. R-134a was intentionally withdrawn since the operating pressure was above the pressure of maximum enthalpy.

Fluid	butane	Geo-only	Hybrid
$\dot{m}$ (kg/s)	58.6	$T_{\text{evap}}$ (°F) 172.1	$T_{\text{evap}}$ (°F) 277.1
x	28.4%	$T_{\text{cond}}$ (°F) 91.5	$T_{\text{cond}}$ (°F) 91.5

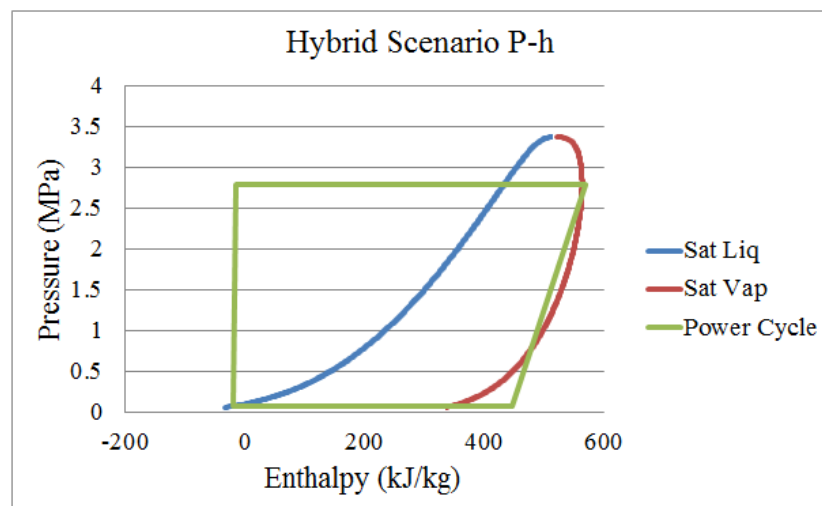
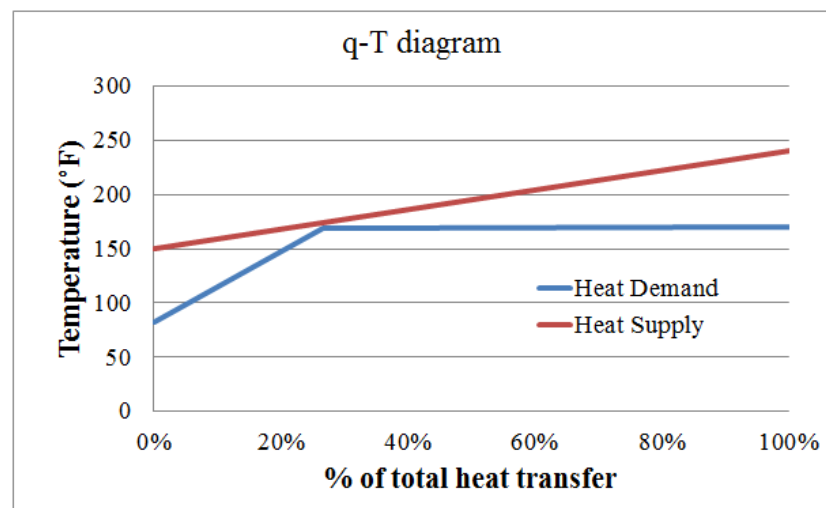
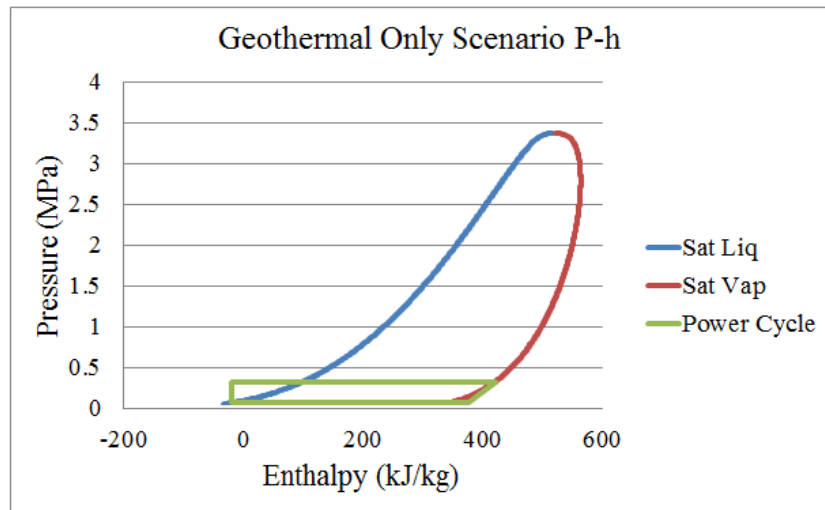


Fluid	isobutane	Geo-only	Hybrid
$\dot{m}$ (kg/s)	58.0	$T_{\text{evap}}$ (°F) 180.5	$T_{\text{evap}}$ (°F) 246.8
x	63.7%	$T_{\text{cond}}$ (°F) 76.0	$T_{\text{cond}}$ (°F) 76.0

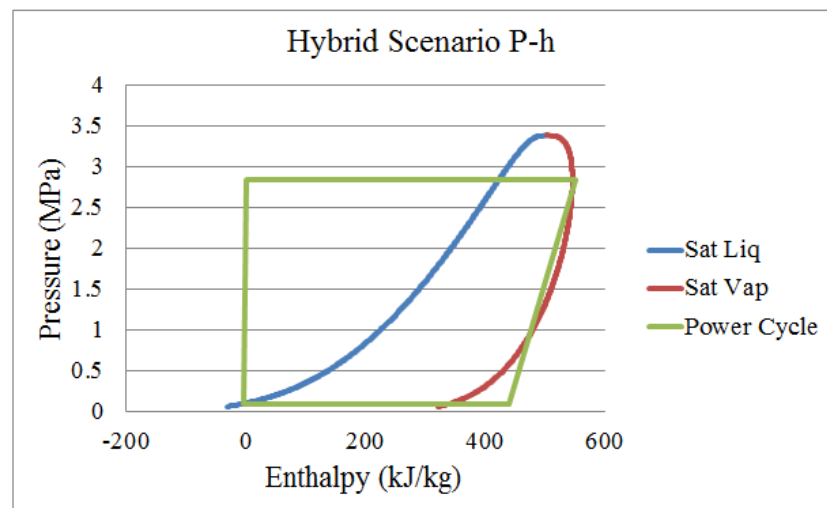
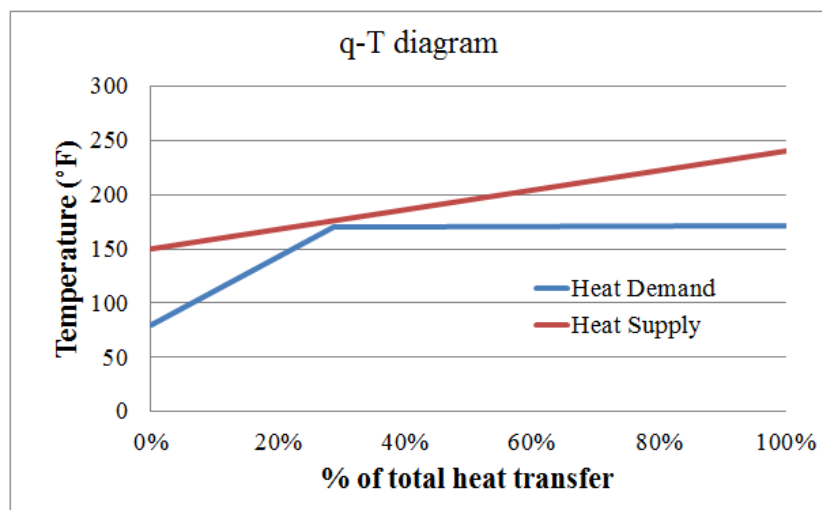
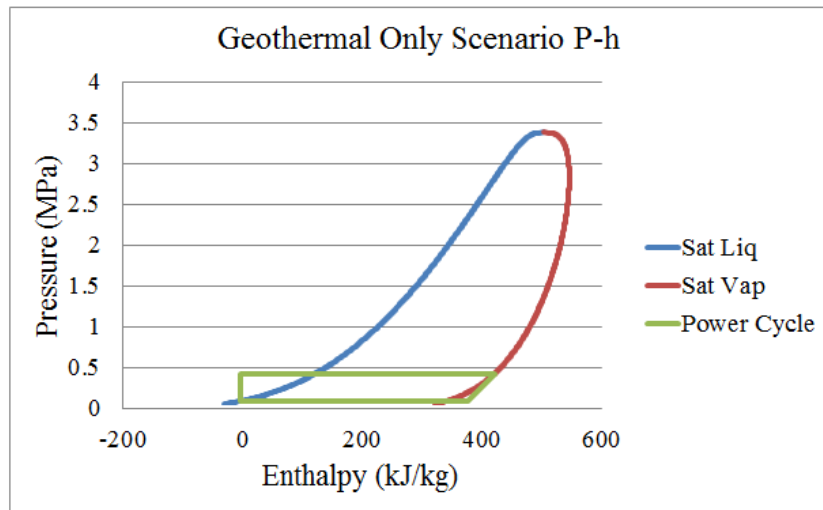




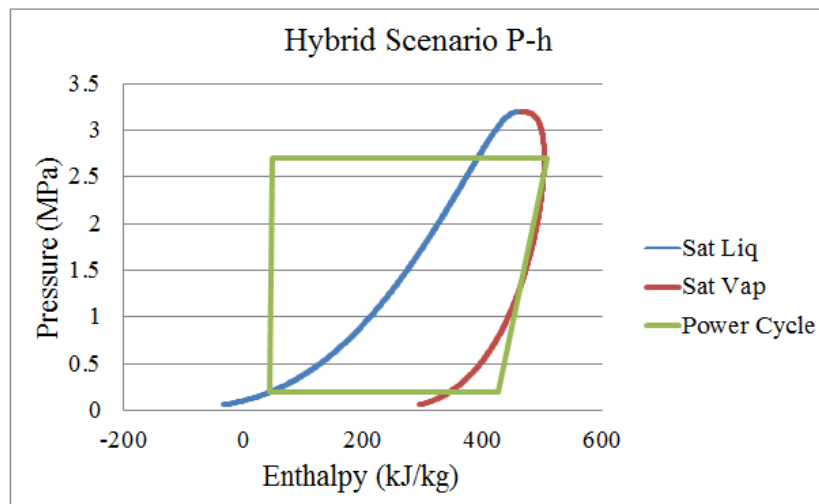
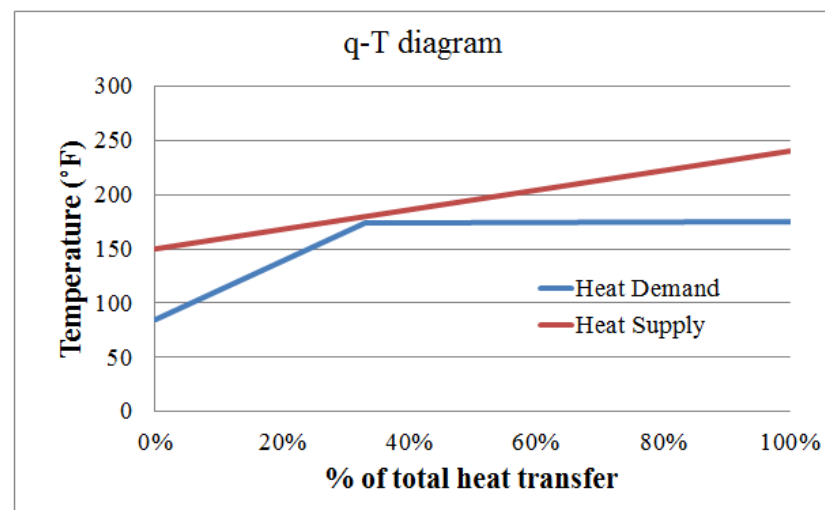
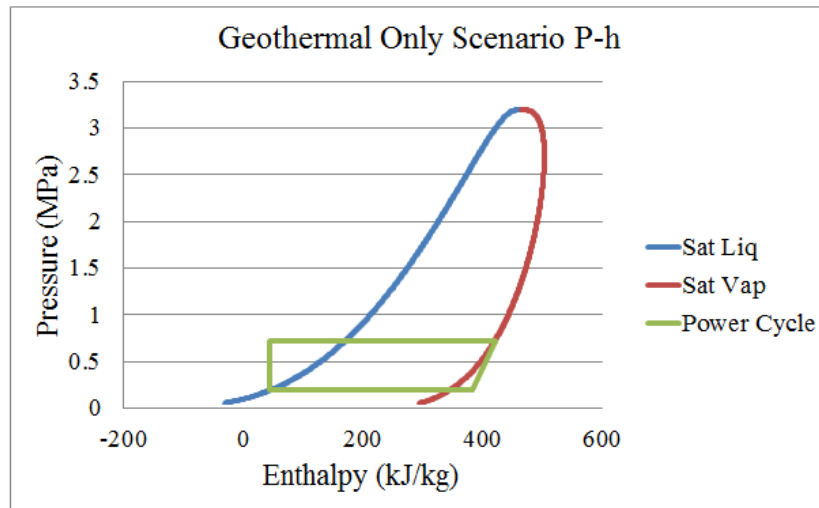
Fluid	pentane	Geo-only	Hybrid
$\dot{m}$ (kg/s)	56.2	$T_{\text{evap}}$ (°F) 168.5	$T_{\text{evap}}$ (°F) 363.8
x	26.6%	$T_{\text{cond}}$ (°F) 82.1	$T_{\text{cond}}$ (°F) 82.1



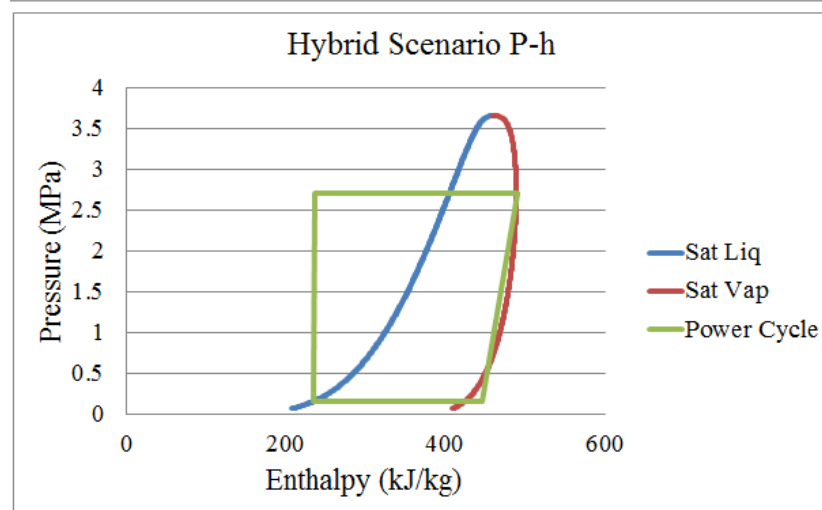
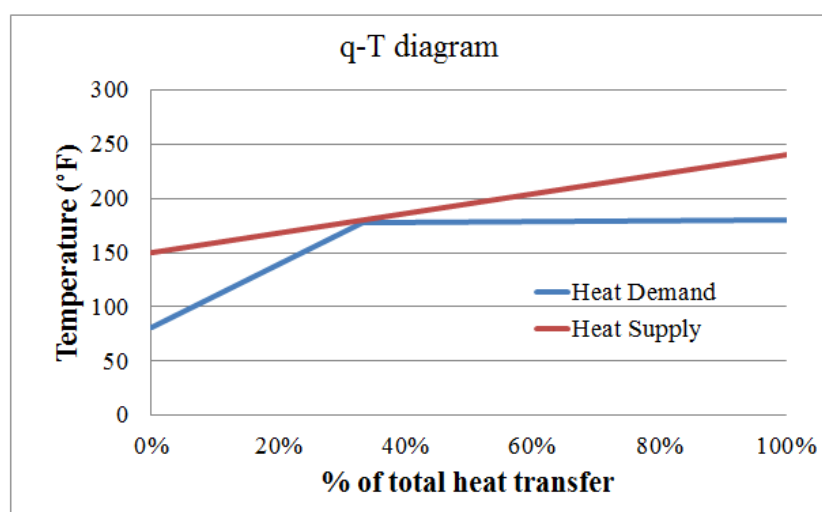
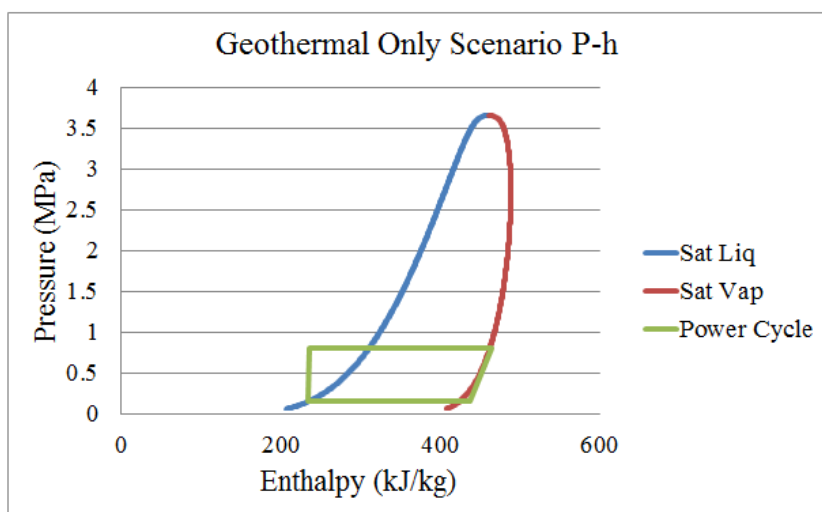
Fluid	isopentane	Geo-only	Hybrid
$\dot{m}$ (kg/s)	59.2	$T_{\text{evap}}$ (°F) 169.8	$T_{\text{evap}}$ (°F) 348.3
x	28.7%	$T_{\text{cond}}$ (°F) 79.6	$T_{\text{cond}}$ (°F) 79.6



Fluid	neopentane	Geo-only	Hybrid
$\dot{m}$ (kg/s)	68.0	$T_{\text{evap}}$ (°F) 173.8	$T_{\text{evap}}$ (°F) 302.0
x	33.1%	$T_{\text{cond}}$ (°F) 83.8	$T_{\text{cond}}$ (°F) 83.8



Fluid	r245fa	Geo-only	Hybrid
$\dot{m}$ (kg/s)	107.2	$T_{\text{evap}}$ (°F) 178.2	$T_{\text{evap}}$ (°F) 279.8
x	33.3%	$T_{\text{cond}}$ (°F) 80.3	$T_{\text{cond}}$ (°F) 80.3



## BIBLIOGRAPHY

- Allred, J. (2004, December). Milgro Greenhouses Newcastle, Utah. *Milgro Greenhouses Newcastle, Utah*. Utah Energy Office.
- Blackett, R. E. (1990). *The Newcastle Geothermal System Iron County, Utah Geology, Hydrology, and Conceptual Model Volume 1: Final Report*. Salt Lake City: Utah Department of Natural Resources Geological and Mineral Survey.
- Blackett, R. E. (2004). *Newcastle, Utah Small-Scale Geothermal Power Development Project - Exploratory Drilling*. Salt Lake City: Utah Department of Natural Resources.
- Blackett, R. E. (2007). *Temperature-Depth Monitoring in the Newcastle Geothermal System*. Salt Lake City: Utah Department of Natural Resources.
- BrightSource. (2011, January 11). *BrightSource*. Retrieved from BrightSource: <http://www.brightsourceenergy.com/projects/ivanpah>
- Calpine. (2011, December 28). *Calpine*. Retrieved December 28, 2011, from The Geysers: <http://www.geysers.com/history.htm>
- Çengel, Y. A. (2006). *Thermodynamics An Engineering Approach 5th Edition*. New York: McGraw-Hill.
- Chapman, D. S. (1981). Thermal Regime of the Escalante Desert, Utah, With an Analysis of the Newcastle Geothermal System. *Journal of Geophysical Research*, 11,735-11,746.
- DeLaquil, P. (1991). Solar One Conversion Project. *Solar Energy Materials*, 151-161.
- DiPippo, R. (2004). Second Law assessment of binary plants generating power from low-temperature geothermal fluids. *Geothermics*, 565-586.
- DiPippo, R. (2007). Ideal thermal efficiency for geothermal binary plants. *Geothermics*, 276-285.
- DiPippo, R. (2008). *Geothermal Power Plants - Principles, Applications, Case Studies and Environmental Impact*. Burlington, MA: Elsevier Ltd.

- Enerdata. (2012, January 1). *Enerdata*. Retrieved January 5, 2012, from Global Energy Statistical Yearbook 2011: <http://yearbook.enerdata.net/>
- European Commission Joint Research Centre. (2007, January 1). *PVGIS Solar Irradiance Data*. Retrieved from PVGIS Solar Irradiance Data: <http://sunbird.jrc.it/pvgis/apps/radday.php?lang=en&map=europe>
- Fernandez-Garcia, A. (2010). Parabolic-trough solar collectors and their applications. *Renewable and Sustainable Energy Reviews*, 1965-1721.
- Forristall, R. (2003). *Heat Transfer Analysis and Modeling of a Parabolic Trough Solar Receiver Implemented in Engineering Equation Solver*. Golden: National Renewable Energy Laboratory.
- Geyer, M. (2002). EuroTrough - Parabolic Trough Collector Developed for Cost Efficient Solar Power Generation. Zurich, Switzerland.
- Google. (2011, January 1). *Google*. Retrieved from Google: <http://maps.google.com/>
- Heberle, F. (2010). Exergy based fluid selection for a geothermal Organic Rankine cycle for combined heat and power generation. *Applied Thermal Engineering*, 1326-1332.
- Herrmann, U. (2004). Two-tank molten salt storage for parabolic trough solar power plants. *Energy*, 883-893.
- Huang, T. C. (2010). A study of organic working fluids on system efficiency of an ORC using low-grade energy sources. *Energy*, 35, 1403-1411.
- Incropera, F. P. (2007). *Fundamentals of Heat and Mass Transfer*. Hoboken: John Wiley & Sons, Inc.
- Kolb, G. J. (1991). Insights from the operation of Solar One and their implications for future central receiver plants. *Solar Energy*, 39-47.
- Kongtragool, B. (2003). A review of solar-powered Stirling engines and low temperature differential Stirling engines. *Renewable & Sustainable Energy Reviews*, 131-154.
- Manente, G. (2011). Hybrid Solar-Geothermal Power Generation to increase the Energy Production from a Binary Geothermal Plant.
- Montes, M. (2009). Solar multiple optimization for a solar-only thermal power plant, using oil as heat transfer fluid in the parabolic trough collectors. *Solar Energy*, 2165-2176.

- National Renewable Energy Laboratory. (2010, March 16). *NREL*. Retrieved from NREL: <http://www.nrel.gov/csp/solarpaces/>
- Padilla, R. V. (2011). Heat transfer analysis of parabolic trough solar receiver. *Applied Energy*.
- Reilly, H. E. (2001). *An Evaluation of Molten-Salt Power towers Including Results of the Solar Two Project*. Albuquerque: Sandia National Laboratories.
- Resort, C. H. (2011, January 1). *Chena Hot Sprongs Resort Fairbanks, Alaska*. Retrieved December 19, 2011, from <http://www.chenahotsprings.com/geothermal-power/>
- Saleh, B. (2007). Working fluids for low-temperature organic Rankine cycles. *Energy*, 1210-1221.
- Sandia National Laboratory. (1981). *Cleaning Strategies for Parabolic-Trough Solar Collector Fields; Guidelines for Decisions*. Albuquerque: Sandia National Laboratory.
- Solucar. (2006). *10 MW Solar Thermal Power Plant for Southern Spain*.
- Solutia. (2012, January 1). *Therminol*. Retrieved from Heat Transfer Fluids by Solutia: <http://www.therminol.com/pages/region/na/default.asp>
- Technology, N. I. (2011, December 27). *NIST Chemistry Webbook*. Retrieved December 27, 2011, from NIST Chemistry Webbook: <http://webbook.nist.gov/chemistry/>
- Unione Geotermica Italiana. (2010, January 1). Retrieved from [http://www.unionegeotermica.it/esperimento\\_ginori\\_conti.asp](http://www.unionegeotermica.it/esperimento_ginori_conti.asp)
- Utah Renewable Energy Zone Interactive Map. (2012, January 1). *UREZ*. Retrieved from UREZ: <http://mapserv.utah.gov/urez/>
- Wheeler, R. (2007, January 1). *Wikipedia*. Retrieved from Wikipedia: [http://en.wikipedia.org/wiki/Sterling\\_engine](http://en.wikipedia.org/wiki/Sterling_engine)